



HAL
open science

Constraining the origin of recently deposited particles using natural radionuclides ^7Be and ^{234}Th in deltaic sediments

Junwen Wu, C. Rabouille, Sabine Charmasson, Jean-Louis Reyss, Xavier Cagnat

► To cite this version:

Junwen Wu, C. Rabouille, Sabine Charmasson, Jean-Louis Reyss, Xavier Cagnat. Constraining the origin of recently deposited particles using natural radionuclides ^7Be and ^{234}Th in deltaic sediments. *Continental Shelf Research*, 2018, 165, pp.106-119. 10.1016/j.csr.2018.06.010 . hal-02635532

HAL Id: hal-02635532

<https://hal.science/hal-02635532>

Submitted on 27 May 2020

HAL is a multi-disciplinary open access archive for the deposit and dissemination of scientific research documents, whether they are published or not. The documents may come from teaching and research institutions in France or abroad, or from public or private research centers.

L'archive ouverte pluridisciplinaire **HAL**, est destinée au dépôt et à la diffusion de documents scientifiques de niveau recherche, publiés ou non, émanant des établissements d'enseignement et de recherche français ou étrangers, des laboratoires publics ou privés.



Distributed under a Creative Commons Attribution - NonCommercial - NoDerivatives 4.0 International License

1

2 **Constraining the origin of recently deposited particles using**
3 **natural radionuclides ^7Be and $^{234}\text{Th}_{\text{ex}}$ in deltaic sediments**

4

5 Junwen Wu^{1,2,4}, Christophe Rabouille^{2*}, Sabine Charmasson^{1*}, Jean Louis Reyss², Xavier
6 Cagnat³

7

8 ¹Institut de Radioprotection et de Sûreté Nucléaire (IRSN), PSE-ENV-SRTE Laboratoire
9 de Recherche sur les Transferts des radionucléides au sein écosystèmes Aquatiques
10 (LRTA) Centre IFREMER de Méditerranée, CS 20330, zone portuaire de Brégaillon,
11 83507, La Seyne-sur-Mer Cedex, France

12 ²Laboratoire des Sciences du Climat et de l'Environnement (LSCE), UMR
13 CEA/CNRS/UVSQ and IPSL, Avenue de la Terrasse, 91190, Gif-sur-Yvette, France

14 ³Institut de Radioprotection et de Sûreté Nucléaire (IRSN), PSE-ENV-STEME,
15 Laboratoire de Mesure de la Radioactivité de l'Environnement (LMRE), Bois des Rames,
16 91400 Orsay, France

17 ⁴College of Science, Shantou University, Shantou 515063, China

18

19

20 **ABSTRACT**

21 ^7Be and $^{234}\text{Th}_{\text{ex}}$ activities were determined in sediment cores off the Rhône River
22 mouth (Gulf of Lions), in order to trace the initial transport and deposition of riverine
23 suspended particulate matter (SPM) and evaluate the impact of flood events through 7
24 cruises carried out over the period of 2007-2008. Consistently high ^7Be and $^{234}\text{Th}_{\text{ex}}$
25 inventories of 2000-3000 mBq cm⁻² and 3000-5000 mBq cm⁻², respectively, were
26 observed within a ~5 km radius off the Rhône River mouth. Their spatial distributions
27 showed a gradual decrease with increasing distance from the Rhône River mouth, and the
28 decrease in ^7Be was more pronounced than that of $^{234}\text{Th}_{\text{ex}}$, indicating that recent riverine
29 SPM is rapidly deposited in the area located near the river mouth. This area is also
30 characterized by high accumulation rates determined using ^{137}Cs or $^{210}\text{Pb}_{\text{ex}}$. Both ^7Be and
31 $^{234}\text{Th}_{\text{ex}}$ inventories increased in 2008 compared to 2007, and are positively correlated to
32 the cumulated SPM flux for normal and flood discharge. Moreover, the $^7\text{Be}/^{234}\text{Th}_{\text{ex}}$
33 inventory ratio appears to be a potential tracer to identify the dominant influence of
34 recently deposited particles between terrestrial and marine waters. This ratio provides
35 an effective tool to assess river and marine influence: Zone I at a distance inferior to 3.0
36 km, with $^7\text{Be}/^{234}\text{Th}_{\text{ex}}$ inventory ratio over 0.50 (surface area near river mouth ~7 km²) is
37 dominated by riverine particles; in contrast, Zone III at a distance superior to 8.5 km,
38 with $^7\text{Be}/^{234}\text{Th}_{\text{ex}}$ inventory ratio less than 0.10 (surface area off river mouth beyond 150
39 km²) is predominantly under a marine influence. In between, an intermediate area
40 displays a mixed influence, with inputs of riverine and marine origins: the transition Zone
41 II at a distance between 3.0 and 8.5 km, with $^7\text{Be}/^{234}\text{Th}_{\text{ex}}$ inventory ratios between 0.10
42 and 0.50. This zoning could help in further understanding the spreading of
43 particle-reactive contaminants and its initial sedimentary deposition in the Gulf of Lions.

44
45 **Keywords:** ^7Be , ^{234}Th , suspended particulate matter, Rhône River, 2008 flood, Gulf
46 of Lions

47

48

Commenté [s1]: see the text I am not sure we need to say that if you say positively correlated

49 1. Introduction

50 River-dominated ocean margins are among the most biogeochemically dynamic
51 regions of the world ocean and play a dominant role in global biogeochemical cycles
52 (Dagg et al., 2004; McKee et al., 2004; Cai, 2011). These areas are highly efficient filters
53 and transformers of terrestrial materials, and are key interfaces between the continent and
54 the open ocean (Bianchi and Allison, 2009; Chen and Borges, 2009). Most of the river
55 suspended particulate matter (SPM) is deposited in continental margin areas and less than
56 5% reach the deep sea (McKee et al., 2004). The SPM undergoes a suite of processes
57 associated with cycles of deposition and resuspension after its initial discharge under
58 different hydrological conditions (Sanford, 1992), especially during river floods and
59 ocean storms. Consequently, the study of SPM deposition in the coastal zone under
60 different hydrological regimes, such as short-term flood events, would help in
61 understanding the fate of terrigenous pollutants carried by the SPM in river-dominated
62 ocean margins.

63 Natural and artificial radionuclides have been widely used to investigate various
64 processes in estuarine, coastal and marine environments (e.g., Santschi et al., 1999;
65 Yeager et al., 2004; Moore and Oliveira, 2008; Su et al., 2011). Generally, flood events
66 occur over very short time-scales (from days to weeks); therefore, radionuclides with
67 short half-lives, such as ^7Be ($t_{1/2}=53.3$ days) and ^{234}Th ($t_{1/2}=24.1$ days), appear to be
68 appropriate tracers for studying flood deposition processes at these short time scales
69 (Feng et al., 1999a; Saari et al., 2010). Resuspension may play a role in redistributing the
70 original deposition and may mix sediments from different origins and age (Ogston et al.,
71 2008).

72 Beryllium-7 (^7Be) is produced by cosmic ray spallation of nitrogen and oxygen in
73 the atmosphere. ^7Be is a particle-reactive element and its distribution coefficient (K_d , L/kg)
74 is estimated to be $\sim 10^5$ in estuarine and coastal waters (Dibb and Rice, 1989; Baskaran
75 and Swarzenski, 2007). Following its formation in the stratosphere and troposphere, ^7Be
76 is scavenged by submicron aerosol particles and is delivered to land principally through
77 precipitation and dry deposition (Lal et al., 1958; Wallbrink and Murray, 1994) and then
78 to rivers through watershed washout (Matisoff et al., 2002). ^7Be is generally used to study
79 various processes over short time-scales, such as soil redistribution and erosion rates,

80 sediment residence time and transport in coastal and estuarine systems (Dibb and Rice,
81 1989; Sommerfield et al., 1999; Taylor et al., 2013). Another highly particle-reactive
82 element, Thorium-234 (^{234}Th), with K_d up to $\sim 10^5$ - 10^6 (Guo et al., 1995; IAEA, 2004;
83 Baskaran and Swarzenski, 2007), is produced from the decay of dissolved ^{238}U and is
84 commonly present in excess (ex) of its parent ^{238}U in coastal suspended matter and
85 bottom sediments (Aller and Cochran, 1976). ^{238}U concentrations in rivers and oceans
86 vary generally linearly with salinity (Skwarzec, 1995). The average ^{238}U concentrations
87 are $41.5 \pm 2.5 \text{ Bq m}^{-3}$ ($3.3 \pm 0.2 \mu\text{g L}^{-1}$) in the open ocean (salinity normalized to 35.00 ‰)
88 and $3.7 \pm 0.4 \text{ Bq m}^{-3}$ ($0.3 \pm 0.03 \mu\text{g L}^{-1}$) in the major world rivers (Ku et al., 1977; Mangini
89 et al., 1979; Owens et al., 2012). Therefore, the production of ^{234}Th is generally greater in
90 the seaward portion of the estuary than that in the landward part (Feng et al., 1999b).
91 Furthermore, due to their short half-lives, ^7Be and ^{234}Th have proven to constitute a
92 couple of excellent tracers to discern short-term variations in estuarine systems, such as
93 flood deposition (Sommerfield et al., 1999; Mullenbach et al., 2004; Palinkas et al., 2005)
94 and dynamic processes of particles and sediments (Olsen et al., 1986; Wallbrink and
95 Murray, 1996; Feng et al., 1999a; Palinkas et al., 2005).

96 The Rhône subaqueous delta is a wave-dominated delta with micro-tidal influence
97 and a pro-grading sedimentary structure (Syvitski and Saito, 2007), where resuspension
98 occurs below 20 meters depth during large southeast storms occurring mostly in winter
99 (Ulises et al., 2008; Dufois et al., 2014). Over the last two decades, numerous studies have
100 been carried out to better understand the fate of particulate discharge from the Rhône
101 River, especially during floods, in supplying terrigenous and river-borne material to the
102 Mediterranean Sea and the flood impact on various processes (e.g., Milliams and Rose,
103 2001; Perianez, 2005; Maillet et al., 2006; Miralles et al., 2006; Lansard et al., 2007;
104 Drexler and Nittrouer, 2008; Cathalot et al., 2010; Fanget et al., 2013). They revealed that
105 a large majority of river particles discharged into the Mediterranean Sea are deposited,
106 biogeochemically transformed and buried close to the Rhône River mouth in the pro-delta
107 area. The transport and deposition of the remaining SPM is mainly diverted to the
108 southwest in the Rhône River plume. Aloisi et al. (1979) showed that SPM derived by the
109 Rhône towards the sea is stratified in a multi-layered system (surface plume, intermediate
110 and benthic nepheloid layers). The surface plume can spread over several kilometers off

111 the river mouth during floods (Naudin et al., 1997; Thill et al., 2001). The intermediate
112 layers are mainly seasonal while the benthic nepheloid layer is the thickest layer, which
113 nourishes the prodelta, shelf and slope. Therefore, defining the preferential deposition
114 area of river-borne particles and its initial repository is of particular interest to better
115 understand the dynamics of riverine particles and their associated contaminants drained
116 by the Rhône River towards the Mediterranean Sea (Charmasson, 2003; Eyrolle et al.,
117 2004; Roussiez et al., 2006, Radakovich et al., 2008).

118 The objective of our study is to define these initial particle deposition areas close to
119 the Rhône River mouth labelled by ^7Be and ^{234}Th tracers, and to improve the
120 understanding of short-term sedimentary processes in this area. It is important to
121 document and understand the short-term deposition of riverine particles as it is strongly
122 linked to the fate of the most labile part of the organic matter and the associated
123 contaminants in these key regions at the land-sea interface constituted by river deltas.

124

125 **2. Materials and methods**

126 **2.1. Study area**

127 The Rhône River, one of the largest rivers in France by its freshwater discharge, has
128 a catchment area of about 98 000 km² and 832 km length and originates from the Alps. It
129 discharges in the Gulf of Lions (NW Mediterranean Sea) through a delta that comprises
130 two branches, Grand Rhône (carrying 90% of the mean water discharge) and Petit Rhône
131 (carrying the remaining 10%) (Ibanez et al., 1997). The Rhône River is the major supplier
132 of freshwater, sediments and nutrients to the Gulf of Lions and the western Mediterranean
133 basin (De Madron et al., 2000; Sempéré et al., 2000; Pont et al., 2002; Sadaoui et al.,
134 2016). The mean annual river discharge was approximately 1720 m³ s⁻¹ in the past sixty
135 years. The values for the 1-year, 2-year, 10-year, 50-year, and 100-year return period (an
136 estimate of the frequency of river flood based on a stochastic concept) of high discharge
137 correspond to 4000, 5000, 8400, 10400 and 11200 m³ s⁻¹, respectively (Eyrolle et al.,
138 2012 and references therein). The annual sediment discharge ranged from 0.98 to 19.7
139 million tons (Mt, 1Mt=1×10¹² g), with a mean discharge of 6.7 Mt over the period
140 1967-2008 (Pont et al., 2002; Eyrolle et al., 2012). Most of the solid load (>80%) is
141 supplied during flood events initiated in the mountainous portions of the Rhône River

142 catchment (Pont et al., 2002; Antonelli et al., 2008). The Gulf of Lions where the Rhône
143 discharges is micro-tidal with tidal range of 30-50 cm (Dufois et al., 2008). Therefore, the
144 Rhône estuary is stratified and tidal mixing is insignificant. A large turbid plume of one
145 meter in thickness (occasionally up to 5 meters) with mixed freshwater and seawater
146 extends offshore towards the southwest (Many et al., 2018). Below this layer, the salinity
147 of the water is the Mediterranean seawater salinity, i.e., 38 ‰. As mentioned above, large
148 resuspension events are limited to the winter and are generally weaker during spring,
149 summer and fall, although occasional storms may displace centimetric layers of sediment
150 (Toussaint et al., 2014; Dufois et al., 2014). The seafloor bathymetry in the subaqueous
151 delta shows three major domains: the proximal domain, in a radius of 2 km off the river
152 mouth with water depth of 10-30 m; the pro-delta domain, 2-5 km off the river mouth
153 with water depth ranging from 30 to 70 m; and the distal domain (continental shelf),
154 beyond 5 km off the river mouth with water depth between 70 and 90 m (Got and Aloisi,
155 1990). The subaqueous delta structure is characterized by fine-grained deposits in the
156 proximal area below 20 meters depth (Durrieu de Madron et al., 2000; Roussiez et al.,
157 2005). The net sedimentation rates varied from 30 to 50 cm yr⁻¹ in the proximal domain
158 (Calmet and Fernandez, 1990; Charmasson et al., 1998), to 1-2 cm yr⁻¹ in the prodelta,
159 down to 0.1-0.6 cm yr⁻¹ with a mean rate of 0.3 cm yr⁻¹ in the distal domain (Radakovitch
160 et al., 1999; Miralles et al., 2005). The grain size in the entire area is quite homogeneous
161 (D_{0.5} =10-15µm) (Bonifacio et al., 2014; Cathalot et al., 2010). The biogeochemical
162 characteristics are also very different between the three zones with large mineralization of
163 organic matter involving sulfate reduction in the proximal and prodelta zones and suboxic
164 diagenesis in the distal region (Pastor et al., 2011; Rassmann et al., 2016).

165 **2.2. River discharge and SPM data**

166 The Rhône River flow was provided by the CNR (*Compagnie Nationale du Rhône*)
167 and SPM was measured at the Arles-SORA station by the MIO (*Mediterranean Institute*
168 *of Oceanology*). Daily SPM samples were obtained by collecting automatically 150 mL
169 of water every 90 min. Samples for SPM analysis were preserved with HgCl₂ and stored
170 at 5 °C until the bulk sample volumes were filtered using 1-µm pre-conditioned glass
171 fiber filters (ashed at 450 °C for 4 h and pre-weighed before filtration). The SPM was
172 quantified by differential weighing after drying at 60 °C for 24 h. The analytical

173 uncertainty of SPM concentrations was 5×10^{-4} g L⁻¹.

174 2.3. Sample collection

175 The sediment cores were collected using various corers with 20-40 cm of length
176 that allow good preservation of the interface, i.e., Usnel box-corers, Ronanberg corer and
177 Octopus multi-corer, during seven cruises conducted in the Gulf of Lions from March 13,
178 2007 to December 7, 2008 (Figure 1), a period characterized by a large and unusual flood
179 in May-June 2008 created by a dam release on the largest alpine tributary (Durance) and
180 a more typical flood in November 2008. Before the May-June 2008 flood, 21 sediment
181 cores were collected in March, April and September 2007, and in March 2008. Five
182 sediment cores were sampled off the Rhône River mouth during the 2008 flood
183 (May-June), but only one core, Stn.AK3, was sampled after the main deposition event in
184 the pro-delta. After the 2008 flood, six stations were sampled in October and December
185 2008. The detailed sample information is listed in Table 1. The sediment core samples
186 were extruded onboard and sliced at depth intervals of 0.5-, 1.0- or 2.0-cm. Then, the
187 subsamples were frozen and kept in that state until they were shipped to the shore-based
188 laboratory, where they were dried (either at 60 °C for 24 h or freeze-dried) and pulverized
189 using agate mortar and pestle sets.

190 2.4. ⁷Be isotope measurement

191 The radionuclide measurements were carried out in two laboratories: “*Laboratoire*
192 *Souterrain de Modane* (LSM)” in the French Alps (Reyss et al., 1995; Cazala et al., 2003)
193 and “*Laboratoire de Mesure de la Radioactivité de l’Environnement* (LMRE)” in Orsay
194 (IRSN) (De Vismes Ott et al., 2013). At LSM, aliquots of 3-4 g were measured in the
195 wells of very low-background and high-efficiency germanium detectors. Protected from
196 cosmic radiation by 1700 m of rocks, a background as low as 0.5 counts per minute from
197 40 keV to 3000 keV was measured. Due to the short half-life, no standard for ⁷Be was
198 used at LSM and the efficiency-versus-energy curve was extrapolated between ¹³⁷Cs
199 gamma ray at 662 keV and ⁴⁰K at 1460 keV to the 478 keV peak of ⁷Be (Larsen and
200 Cutshall, 1981). Generally, a counting time of one day for the deepest samples leads to
201 precise data (uncertainty less than 10% for 2σ counting statistical error). At LMRE, 60
202 mL or 220 mL (~50-300 g) sediments were measured with the coaxial or semi-planar
203 (HPGe) germanium detectors for 24-48 hours, with a relative efficiency greater than 50%.

Commenté [s2]: if my memroy is correct with this corer we sampled cores about 60 to 80cm length, right?

Mis en forme : Anglais (États-Unis)

204 Detectors were in a room shielded with 10 cm of low-background lead and 5 mm of
205 electrolytic copper, located underground under a 3-m-thick boron concrete slab (De
206 Vismes Ott et al., 2013). Calibrations in energy, resolution and efficiency were carried out
207 using standard sources (including ^7Be) prepared in the “*Laboratoire des Etalons et*
208 *Intercomparaisons*” of the IRSN (LEI, under COFRAC accreditation), filled with an
209 epoxide resin multi-gamma mixture source supplied by CERCA Inc (France). The ^7Be was
210 measured via its peak at 477 keV of 10.44% emission intensity. Activities of ^7Be were all
211 corrected for decay since the date of sample collection in this study, and expressed as Bq
212 kg^{-1} of dry weight of sediment. The two laboratories regularly participate in
213 inter-comparison exercises at national and international levels and are reference
214 laboratories in France. The results show an overall agreement between the two techniques
215 with less than 10% difference.

216 2.5. $^{234}\text{Th}_{\text{ex}}$ isotope analysis

217 The dried and homogenized samples were weighed and transferred to plastic
218 counting geometries for non-destructive analysis of ^{234}Th using gamma spectrometry. At
219 LSM, six standards were used to calibrate the gamma detectors for the determination of
220 gamma emitters (Cazala et al., 2003). ^{234}Th activity was measured in both laboratories
221 directly from its gamma photo-peak at 63.3 keV. A correction for gamma attenuation was
222 applied and the self-adsorption coefficient for ^{234}Th was also determined according to the
223 methods suggested by Cutshall et al. (1983), because significant self-absorption of
224 gamma energy occurs below 295 keV. At LMRE, for this low-energy line (<100 keV), a
225 transmission measurement was carried out to determine the attenuation coefficients of the
226 samples in order to correct the measured activity of the self-attenuation phenomena, which
227 may be significant for sediments, especially on large geometries (220 mL) (Lefèvre et al.,
228 2003). In addition, ^{234}Th supported by its grandparent ^{238}U was determined by recounting
229 those samples at depth in the core after approximately 5 months. The average activities
230 measured in the second count were subtracted from the activities determined in the first
231 counting session. This allows us to determine excess ^{234}Th activities (activities not
232 supported by ^{238}U ; denoted $^{234}\text{Th}_{\text{ex}}$). The counting time was at least 24 h, depending on
233 the sample activity. The activities of the excess ^{234}Th ($^{234}\text{Th}_{\text{ex}}$) were all corrected for
234 decay since the sampling date and expressed as Bq kg^{-1} of dry weight of sediment.

235 **2.6. Calculation of ^7Be and $^{234}\text{Th}_{\text{ex}}$ inventories and SPM flux**

236 Inventories of ^7Be and $^{234}\text{Th}_{\text{ex}}$ are useful parameters for assessing the deposition
237 process of SPM. In this study, ^7Be and $^{234}\text{Th}_{\text{ex}}$ inventories in dry sediments were
238 calculated by summing their respective activities at each layer, according to the following
239 formula (Wang and Yamada, 2005):

240
$$I = \sum_{i=1}^N \rho_s X_i A_i \quad (1)$$

241 where I represents the inventories of ^7Be or $^{234}\text{Th}_{\text{ex}}$ in the dry sediments (mBq cm^{-2}),
242 N is the number of sampling layers, ρ_s is the solid phase dry density, X is the
243 thickness of the sampling interval i (cm), and A is the activity of the sampled interval
244 (Bq kg^{-1}). Uncertainties on inventories are the sum of the propagated error determined for
245 each of the sampling intervals. In some cores, ^7Be or $^{234}\text{Th}_{\text{ex}}$ activities were still detected
246 in the deepest sampled layers. Therefore, for these cores the activities in the un-sampled
247 deepest layers were extrapolated by the use of an exponential equation fitted to the
248 existing field data, to allow estimates of completed (closed) inventories.

249 The annual SPM fluxes (SPM_a in kg) were calculated through the following
250 equation (Eyrolle et al., 2012):

251
$$\text{SPM}_a = \sum_{t=1}^{t=n} ((\text{SPM}_{ct} + \text{SPM}_{ct+1}) / 2) \cdot ((Q_t + Q_{t+1}) / 2) \cdot \Delta T \quad (2)$$

252 where n is the number of samples collected during the year, SPM_{ct} represents the SPM
253 concentration measured over a given period of time or at the time t (mg L^{-1}), Q is the
254 average river flow during the sampling period ($\text{m}^3 \text{s}^{-1}$), and ΔT is the period of time
255 between two continuous samples collected at times t and $t+1$ (s). In order to take into
256 account the fact that sediment deposition integrates several deposition events, and to
257 better link particulate inputs and sediment inventories on the same timescale, we also
258 calculated the cumulated SPM fluxes over two half-lives before the sampling date for
259 each radionuclide by summing the particle discharge over this period of time, namely,
260 ~ 106 d for ^7Be and ~ 48 d for ^{234}Th . For time periods longer than two half-lives before the
261 sampling period, the radionuclide inventory will have decreased by 75% and will
262 contribute marginally to the overall inventory.

263 **3. Results**

264 **3.1. Temporal variations of river flow rates and particulate discharge**

265 Temporal variations of river flow rates and particulate discharges measured at the
266 SORA station located on the Grand Rhône in Arles 40 km upstream of the river mouth
267 during the period 2007-2008 are presented in [Figure 2](#). The mean annual river flow rate
268 over our study period is $1566 \pm 834 \text{ m}^3 \text{ s}^{-1}$, which is in the range of the mean value over
269 the past sixty years ($1720 \pm 982 \text{ m}^3 \text{ s}^{-1}$). At the SORA station in Arles, a river flood event is
270 defined as a river flow rate above $3000 \text{ m}^3 \text{ s}^{-1}$ since this threshold corresponds to a
271 breakdown in the relationship between the river flow and SPM concentrations indicating
272 the initiation of sediment transport under flood conditions ([Pont et al., 2002](#); [Antonelli,](#)
273 [2002](#); [Eyrolle et al., 2012](#)). The year 2007 was defined as a “no flood” year with river
274 flow only approaching or slightly exceeding $3000 \text{ m}^3 \text{ s}^{-1}$ in March 4-9 and on November
275 24 ([Figure 2a](#)) and was characterized by a very low annual particulate discharge, i.e., 1.5
276 Mt. In contrast, the year 2008 was characterized by a succession of moderate floods with
277 maxima of about $4000\text{-}5000 \text{ m}^3 \text{ s}^{-1}$ ([Eyrolle et al., 2012](#); [Zebracki et al., 2015](#)). Over our
278 2008 sampling period (ending on December 7, 2008), two main floods occurred ([Figure](#)
279 [2b](#)): the first and main one in terms of duration started on May 28 and ended on June 12,
280 2008 (~16 d), and the second one occurred between November 2-7, 2008 (~6 d).
281 However, the SPM concentrations observed in May-June 2008 are exceptionally high for
282 such a moderate flood. A mean daily SPM concentration peak reaching 3356 mg L^{-1} was
283 recorded on June 1, 2008, with daily maximum SPM fluxes reaching 11940 kg s^{-1} . It is
284 estimated that this atypical flood event of anthropogenic origin induced the transfer of 4.7
285 Mt SPM towards the sea over a 16 day period, mostly from the flushing of old sediment
286 trapped in reservoirs and the erosion of the river banks, which contains unusually low
287 short-lived radionuclides ([Eyrolle et al., 2012](#)) and old carbon ([Cathalot et al., 2013](#)). This
288 flood event accounts for ~52% of the 2008 annual SPM fluxes (about 9.1 Mt) and
289 represents by itself three times the 2007 annual SPM fluxes (~1.5 Mt) ([Eyrolle et al.,](#)
290 [2012](#)). In contrast, the SPM flux (~0.4 Mt) induced by the November flood event that
291 reached $4800 \text{ m}^3 \text{ s}^{-1}$ (November 2-7, 2008) only accounted for ~4% of the 2008 annual
292 SPM flux (Grand Rhône).

293 **3.2. ^7Be activities and inventories**

294 A selection of vertical distributions of ^7Be activities in the sediment cores are shown
295 in Figure 3. Depth profiles of ^7Be activities in the sediment cores showed an overall
296 decrease with depth, which is caused by burial, bioturbation and gradual decay of ^7Be
297 with depth (Fitzgerald et al., 2001; Miralles et al., 2006). The ^7Be penetration depth also
298 shows a decrease with increasing distance from the river mouth (from Stn.A to Stns. B, C,
299 D, E and U).

300 Distributions of ^7Be activities in surface sediments demonstrate spatial and temporal
301 variations. Spatial distributions showed a clear decrease of surface ^7Be activity with
302 increasing distance from the river mouth. For example, in April 2007, along the SW
303 direction, ^7Be activities at Stn.A adjacent to the river mouth were higher than at Stns. B,
304 N and E.

305 ^7Be inventories in the sediment cores are listed in Table 2 and they showed a large
306 spatial variation with a 85-fold decrease from Stn.A in May 2008 (1826 mBq cm^{-2}) to
307 Stn.U on the shelf (21 mBq cm^{-2}).

308 3.3. $^{234}\text{Th}_{\text{ex}}$ activities and inventories

309 Vertical distributions of $^{234}\text{Th}_{\text{ex}}$ activities in sediment cores also showed a decrease
310 with increasing depth (Figure 4). However, the horizontal distribution of surface activity
311 is inconsistent with that of ^7Be , since the $^{234}\text{Th}_{\text{ex}}$ activities in surface sediments did not
312 show a decrease with distance from the river mouth. Along the SW direction, the $^{234}\text{Th}_{\text{ex}}$
313 activity at Stn.E was higher than that of Stn.B close to the river mouth in April 2007.

314 $^{234}\text{Th}_{\text{ex}}$ inventories in the sediment cores are also listed in Table 2. They varied from
315 525 to 5474 mBq cm^{-2} , showing a 10-fold decrease along the offshore transect. Within a 3
316 km area at the river mouth, $^{234}\text{Th}_{\text{ex}}$ inventories along the increasing distance from the
317 river mouth varied from $2042 \pm 668 \text{ mBq cm}^{-2}$ at Stn.A (2.1 km) to $1294 \pm 292 \text{ mBq cm}^{-2}$ at
318 Stn.B (2.9 km) in April 2007. During the same period, $^{234}\text{Th}_{\text{ex}}$ inventory ($856 \pm 89 \text{ mBq}$
319 cm^{-2}) at Stn.E (16.6 km) appears only slightly higher compared to Stn.N ($599 \pm 196 \text{ mBq}$
320 cm^{-2}) closer to the coast (5.1 km). When considering their uncertainty, $^{234}\text{Th}_{\text{ex}}$ inventories
321 do not demonstrate a clear spatial variation as can be seen on ^7Be inventory distribution.
322 This has to be related to the differences in primary sources: a point source from the mouth
323 for ^7Be , while $^{234}\text{Th}_{\text{ex}}$ source is more spread out since it is produced in situ from dissolved
324 uranium in saline water.

325

326 **4. Discussion**

327 **4.1. ^7Be and $^{234}\text{Th}_{\text{ex}}$ as tracers of short term SPM deposition**

328 SPM concentrations in surface water decrease rapidly seaward from 20 mg L⁻¹ near
329 the Rhône River mouth to 1.5 mg L⁻¹ at the shelf break (Many et al., 2016). Given that
330 ^7Be is largely associated with riverine particles, it thus follows the main riverine SPM
331 deposition patterns. Therefore, the clear decrease in ^7Be activities with distance from the
332 Rhône River mouth can be associated with the decreasing contribution of river-borne
333 particles in offshore sediments. ^7Be inventories also showed an exponential decrease with
334 increasing distance from Rhône River mouth to shelf (seaward). The ^7Be inventories
335 reach low values when the distance is over 5 km (see Figure 5a) and the highest ^7Be
336 inventories appear within a ~5 km radius from the Rhône River mouth due to higher
337 activities and sediment penetration, indicating an important deposition of recent particles
338 at these locations. The lower ^7Be inventories determined in sediments beyond 5 km off
339 the river mouth indicate lower deposition rates or deposition of aged resuspended
340 particles. Previous observations of the diffusive oxygen fluxes into the sediment (Lansard
341 et al., 2009; Rassmann et al., 2016), organic carbon contents and chlorophyll-a
342 concentrations in surficial sediments (Cathalot et al., 2010; Bourgeois et al., 2011) and
343 other organic tracers (Cathalot et al., 2013) indicated similar gradients: the labile organic
344 matter is deposited and mineralized near the river mouth creating larger oxygen demand,
345 and concentrations of chlorophyll-a with younger ^{14}C ages of organic matter whereas
346 shelf sediments were characterized by lower oxygen demands and older organic material.
347 In addition, we point out the variability in the ^7Be inventories obtained at Stn.A in March
348 2007 (847 to 1915 mBq cm⁻²) (Table 2). This variability could be due to the fact that
349 these cores were sampled in a channelized area characterized by high spatial variability in
350 transport mechanisms (Maillet et al., 2006). Notwithstanding the variability at station A,
351 the gradient between the proximal zone and the continental shelf is still very large with a
352 50-fold decrease between the station A at lowest value and the station U. It should also be
353 noted that our two years study did not include many winter periods where significant
354 resuspension events occur (Ulses et al., 2008).

355 Concerning $^{234}\text{Th}_{\text{ex}}$, high concentrations generally indicate a marine influence as it

356 is produced by the decay of ^{238}U which is enriched in seawater. However, high $^{234}\text{Th}_{\text{ex}}$
357 activities are also observed near the Rhône River mouth. One reason could be the large
358 amounts of riverine particles that would enhance $^{234}\text{Th}_{\text{ex}}$ scavenging from the saline part
359 of the stratified water column at the river mouth (Corbett et al., 2004; McCubbin et al.,
360 2004). Alternatively, the Rhône River could be an additional ^{234}Th source, as dissolved
361 ^{238}U concentrations in the Rhône River are in the range of $7.5\text{-}20.0\text{ Bq m}^{-3}$ ($0.6\text{-}1.6\text{ }\mu\text{g}$
362 L^{-1}). This is 2-5 times larger than the average concentration in the world rivers (3.7 ± 0.4
363 Bq m^{-3} , $0.3\pm 0.03\text{ }\mu\text{g L}^{-1}$) (Ollivier et al., 2011), but lower than the average ^{238}U
364 concentration of seawater in the Mediterranean Sea, which is $\sim 43.2\text{ Bq m}^{-3}$ ($\sim 3.5\text{ }\mu\text{g L}^{-1}$)
365 (Delanghe et al., 2002). These high ^{238}U concentrations in the Rhône River water could
366 be related to the lithological composition (carbonate rocks) of the Rhône basin (Ollivier
367 et al., 2011) and agricultural fertilizers such as phosphates containing high ^{238}U used in
368 the Rhône watershed (Eyrolle et al., 2012). Meanwhile, Zebracki et al. (2017) did not
369 observe $^{234}\text{Th}_{\text{ex}}$ on SPM in the Lower Rhône River at the flow rates above $3000\text{ m}^3\text{ s}^{-1}$.
370 Therefore, the large ^{238}U concentration encountered in the river water allows the river to
371 be a source of ^{234}Th limited to the Rhône prodelta.

372 $^{234}\text{Th}_{\text{ex}}$ inventories show a gradual decrease with increasing distance from the
373 Rhône River mouth, and the highest $^{234}\text{Th}_{\text{ex}}$ inventories are also observed within a $\sim 5\text{ km}$
374 radius off the river mouth (Figure 5b). However, high $^{234}\text{Th}_{\text{ex}}$ inventories are still
375 observed beyond a $\sim 5\text{ km}$ radius off the Rhône River mouth, such as at Stns. C (3000
376 mBq cm^{-2}) and D (2118 mBq cm^{-2}), which is different from the pattern of ^7Be . Such a
377 difference in $^{234}\text{Th}_{\text{ex}}$ and ^7Be inventory distribution can be mainly attributed to their
378 different source terms, i.e., ^7Be source derived mainly from the river, while the $^{234}\text{Th}_{\text{ex}}$ is
379 linked to in situ production in saline water (Saari et al., 2010).

380 4.2. Relation of ^7Be and $^{234}\text{Th}_{\text{ex}}$ with river particulate flux

381 Large temporal variations in ^7Be activities near the river mouth (Stns. A, AB, AK)
382 appeared to be associated with river particulate discharge. In general, high river
383 particulate discharge corresponds to high ^7Be activities in proximal zone sediments. For
384 example, at Stn. A, ^7Be activities in December 2008 were higher than that in March 2008
385 since the river particulate discharge in December 2008 was also higher compared to

Commenté [s3]: right so it is why it is not correct to speak about marine particles idem if the Rhone is a source of ^{234}Th

386 March 2008. Like ^7Be , $^{234}\text{Th}_{\text{ex}}$ activities (Table 2) also seem to demonstrate a positive
387 relation with the river particulate discharge ($R^2=0.26$, $p<0.05$). For example, at Stn.A,
388 $^{234}\text{Th}_{\text{ex}}$ activities (Table 2) observed in March 2007 are higher than in September 2007
389 when the SPM flux is lower.

390 Indeed, at this station, the periods of high ^7Be and $^{234}\text{Th}_{\text{ex}}$ inventories were associated
391 with higher river flow and river particle discharge. Indeed, high SPM riverine fluxes in
392 March 2007 and December 2008 led to higher ^7Be and $^{234}\text{Th}_{\text{ex}}$ inventories compared to
393 those observed in September 2007 and March 2008 when SPM fluxes were lower.

Commenté [r4]: Agreed! This is clearer.

394 (Table 2). This agrees with a study on the western shelf of the Mississippi River
395 delta carried out by Corbett et al. (2007), where high ^7Be inventories near the Mississippi
396 River mouth were positively related to river particulate discharge. Similar time variations
397 of ^7Be and $^{234}\text{Th}_{\text{ex}}$ inventories were also observed in other estuarine systems, such as the
398 Tampa Bay (Baskaran and Swarzenski, 2007), Gironde estuary (Saari et al., 2010) and
399 Yangtze River estuary (Wang et al., 2016).

400 High inventories of short-lived radionuclides in the sediment indicate high recent
401 deposition of particles near the river mouth and most probably preferential deposition and
402 accumulation of sediment. Indeed, apparent accumulation rates studied in the same areas
403 with longer half-life radionuclides such as ^{137}Cs or ^{210}Pb (Calmet and Fernandez, 1990;
404 Charmasson et al., 1998; Radakocitch et al., 1999) also show large sedimentation rates
405 near the Rhône River mouth with very high values around $30\text{-}50\text{ cm yr}^{-1}$ and a gradual
406 decrease with increasing distance from the shoreline. Certainly, this apparent consistency
407 between inventories and apparent accumulation rates does not imply that once settled the
408 bottom particles do not undergo resuspension/transport processes since this area can be
409 very dynamic during storm events, especially during the winter (Marion et al., 2010;
410 Dufois et al., 2014).

411 As we have seen, the activities and inventories of ^7Be and $^{234}\text{Th}_{\text{ex}}$ are only
412 qualitatively related to river particulate discharges. This is due to the integrative timescale
413 of sediment inventory (which spans over a few half-lives of the radionuclides) versus the
414 instantaneous time frame captured by the daily particulate discharge. To bridge this time
415 lag, we have integrated the SPM fluxes over the period preceding the sampling date and

416 compared it to the sediment inventory. The integration period covering two half-lives
417 before the sampling date was chosen, i.e., 106 days for ^7Be and 48 days for $^{234}\text{Th}_{\text{ex}}$ (see in
418 the Materials and Methods section). The cumulated SPM fluxes calculated accordingly
419 are listed in Table 2 and compared with the ^7Be inventory in sediments (Figure 7a).

420 Before discussing the correlations, it is worth noting that the SPM concentration in
421 2008 May-June flood is similar to the December 2003 major flood (3669 mg L^{-1} for a
422 flow rate of about $10000 \text{ m}^3 \text{ s}^{-1}$; Eyrolle et al., 2012). This atypical high particulate load is
423 linked to the upper Durance dam management, which discharged the excess water after
424 heavy precipitation events in the southeastern Rhône watershed (Eyrolle et al., 2012).
425 Therefore, the Stn.AK3 (close to the river mouth and sampled after the May-June flood)
426 is very peculiar due to the nature of the transported solid load, which was characterized as
427 “old” material (Cathalot et al., 2013) consequently depleted in short half-life
428 radionuclides (Eyrolle et al., 2012). Accordingly, the highest cumulated SPM flux
429 corresponds to low short-lived radionuclide activities, resulting in lower inventories than
430 those expected under typical flood conditions (see a broader discussion of this atypical
431 flood in Eyrolle et al., 2012). When data from this atypical flood (Stn.AK3) were
432 excluded, ^7Be inventories show a good correlation with the cumulated SPM flux
433 ($R^2=0.71$, $p<0.05$), indicating that the ^7Be inventory is a fair record of the riverine
434 particles deposition on a timescale of 3-4 months.

435 The highest $^{234}\text{Th}_{\text{ex}}$ inventories were observed in the river mouth, such as at station
436 A. This suggests that: 1) $^{234}\text{Th}_{\text{ex}}$ generated by both seawater and the Rhône water was
437 carried by particles towards the river delta (Ollivier et al., 2011); 2) the scavenging of
438 $^{234}\text{Th}_{\text{ex}}$ was enhanced because freshwater mixing with marine water led to high turbidity
439 and sedimentation rates (aggregation and flocculation processes) in this area. Through
440 12-year observations (1988-2000), Corbett et al. (2004) also pointed out that the $^{234}\text{Th}_{\text{ex}}$
441 inventories in the Mississippi River estuary are positively correlated with river particulate
442 discharge. $^{234}\text{Th}_{\text{ex}}$ inventories also seem to be related to Rhône River particulate discharge
443 although the relation with cumulated SPM fluxes over ~48 days before the sampling
444 appears to be much weaker compared to ^7Be ($R^2=0.44$, $p<0.05$) (Figure 7b). As
445 mentioned above, this is likely linked to their difference in source terms, which are
446 mainly riverine for ^7Be and both riverine and marine for $^{234}\text{Th}_{\text{ex}}$. The ^7Be and $^{234}\text{Th}_{\text{ex}}$

Commenté [s5]: again this shows that you have riverine particles with ^{234}Th

447 particulate activities in the lower Rhône River ranged from 15 to 400 Bq kg⁻¹ and from
448 unquantifiable to 56±14 Bq kg⁻¹, respectively (Eyrolle et al., 2012; Zebracki et al., 2017).
449 Despite the dual nature of ²³⁴Th_{ex}, the different sources allow us to define a zoning with
450 respect to the influence of the Rhône River particulate discharge.

451 **4.3. Zoning of the Rhône River influence on sediments**

452 ⁷Be and ²³⁴Th_{ex} are both strongly bound to particulate matter, without significant
453 difference in preferential adsorption (*K_d*) at high SPM concentrations, such as in the river
454 mouth (Baskaran et al., 1997; Baskaran and Swarzenski, 2007). The potential differences
455 in their specific activities and inventories are mainly caused by source terms, seasonal
456 variations of the river particulate discharge, grain size, distance of salt-water intrusion
457 and amounts of particles in the water column (Feng et al., 1999a; Saari et al., 2010).
458 Figure 5a clearly shows two populations of ⁷Be inventories with large and variable values
459 near the river mouth at stations A and AB (or AZ) which are the closest stations to the
460 river mouth and lower values further on the shelf. It must be noted that the two possible
461 explanations of Figure 5a (i.e. two separate inventory populations or gradual decrease
462 offshore of the inventories) support the zoning based on ⁷Be/²³⁴Th_{ex} inventory. The
463 decrease in ⁷Be inventory offshore is persistent in time and the trend lines for 2007 and
464 2008 show good statistics (R²=0.49 and 0.53) which lend support to a rapid decrease of
465 ⁷Be activity offshore. ⁷Be is thus a powerful tracer for riverine particles although
466 ⁷Be-deficient sediments were exceptionally discharged by the Rhône River to the sea
467 during the May flood event of 2008 due to rapid erosion of old watershed sediments. The
468 situation is less clear for ²³⁴Th_{ex} as a tracer of marine influence with more variable
469 inventory at and near the river mouth, but a decrease offshore, although much weaker
470 than ⁷Be, is also visible (Figure 5b). Notably, this weak decrease of ²³⁴Th inventories
471 from the mouth of the river towards the shelf in the Rhône River deltaic region is
472 contrary to expectations if ²³⁴Th is assumed to have only a marine source. The large
473 spread observed in both radionuclides inventory is due to different source inputs, change
474 in grain size and sediment type (Feng et al., 1999a, b). The use of ⁷Be/²³⁴Th_{ex} inventory
475 ratio may allow avoiding these inventory variations and be a better indicator than ⁷Be
476 alone. It is noteworthy that, in other cases such as the Mississippi River deltaic region
477 where ²³⁴Th_{ex} inventories increase with the distance off the river mouth (Corbett et al.,

478 2004), the use of ${}^7\text{Be}/{}^{234}\text{Th}_{\text{ex}}$ inventory ratio is more powerful than the single radionuclide
479 ${}^7\text{Be}$.

480
481

482 .),

483 The ${}^7\text{Be}/{}^{234}\text{Th}_{\text{ex}}$ inventory ratios in sediment ranged from 0.02 to 0.77, with large
484 variations with the distance from the Rhône mouth (Figure 8). The ${}^7\text{Be}/{}^{234}\text{Th}_{\text{ex}}$ inventory
485 ratios decreased from 0.59 at Stn.A3 (32 m water depth) to 0.04 at Stn.U (90 m water
486 depth) in June 2008, and from 0.77 (21 m water depth) at Stn.A4 to 0.17 at Stn.C (72 m
487 water depth) in December 2008. The lowest ratio of 0.04 indicates that the riverine source
488 traced by ${}^7\text{Be}$ has disappeared and that the marine influence is dominant. In contrast, the
489 high ratio of 0.77 indicates that the riverine source is dominant. High ${}^7\text{Be}/{}^{234}\text{Th}_{\text{ex}}$
490 inventory ratios also mainly occur within a ~ 5 km radius off the river mouth. Feng et al.
491 (1999b) pointed out that the ${}^7\text{Be}/{}^{234}\text{Th}_{\text{ex}}$ inventory ratios are a negative function of both
492 the water depth and salinity in a completely different context of a partially-mixed tidal
493 estuary, namely, increasing with the decrease of water depth and salinity. However, the
494 Rhône River plume spreads over kilometers off the Rhône mouth and the low salinity
495 waters are confined to a thin surface layer at the surface with seawater below the plume
496 (Naudin et al., 1997; Amoux-Chiavassa et al., 2003; Many et al., 2016), indicating that
497 the impact of salinity on ${}^7\text{Be}/{}^{234}\text{Th}_{\text{ex}}$ inventory ratio can be ruled out. Thus, in our case,
498 ${}^7\text{Be}/{}^{234}\text{Th}_{\text{ex}}$ inventory ratio is negatively correlated with water depth.

499 The ${}^7\text{Be}/{}^{234}\text{Th}_{\text{ex}}$ inventory ratios also show temporal variations and are mainly
500 related to river particulate discharge, especially close to the river mouth. The ${}^7\text{Be}/{}^{234}\text{Th}_{\text{ex}}$
501 inventory ratios during 2008 are overall higher than in 2007. The ${}^7\text{Be}/{}^{234}\text{Th}_{\text{ex}}$ inventory
502 ratios also demonstrated an overall positive correlation with the river particulate
503 discharge, from normal discharge to flood discharge. At Stn.A, the ${}^7\text{Be}/{}^{234}\text{Th}_{\text{ex}}$ inventory
504 ratios in December 2008 (influenced by the November flood) are higher than that in
505 March 2008, when the discharges were lower and resuspension during the end of the
506 winter may have redistributed part of the deposited particles. In addition, as already
507 reported, a preferential deposition towards SW is visible in our data set. In this direction
508 at Stn.C (8.5 km away from river mouth), the ${}^7\text{Be}/{}^{234}\text{Th}_{\text{ex}}$ inventory ratios in December

Commenté [s6]: necessary ??? not very clear, if you have a positive relationship it means that high discharge led to high inventories ratios so it is enough not need to add this..

509 2008 were three times larger than that in April 2007, showing that this station is impacted
510 by newly deposited particles. On the contrary, in the SE direction at Stn.L (4.5 km), the
511 ${}^7\text{Be}/{}^{234}\text{Th}_{\text{ex}}$ inventory ratio displays lower values. This feature is clearly consistent with
512 the dominant spread direction of the Rhône River plume, generally in the SW direction,
513 which has been proven to be the preferential direction for deposition of the riverine
514 material in this area (Naudin et al., 1997). Similar patterns have already been reported for
515 other tracers, such as trace metals (Alliot et al., 2003; Roussiez et al., 2006; Radakovitch
516 et al., 2008), man-made radionuclides (Calmet and Fernandez, 1990; Charmasson, 2003;
517 Lansard et al., 2007), and carbon and nitrogen stable isotopes (Lansard et al., 2009;
518 Cathalot et al., 2013).

519 The use of the ${}^7\text{Be}/{}^{234}\text{Th}_{\text{ex}}$ inventory ratio allowed us to establish a zoning
520 regarding the particle deposition with the distance from the Rhône River mouth. In order
521 to examine if ${}^7\text{Be}/{}^{234}\text{Th}_{\text{ex}}$ inventory ratios have a significant difference in the different
522 zones, we applied a simple Mann-Whitney U test (Fay and Proschan, 2010). Close to the
523 Rhône River mouth, at a distance of less than 3.0 km, such as for Stns. A, AB and AK4,
524 defined as Zone I (surface area near river mouth $\sim 7 \text{ km}^2$), ${}^7\text{Be}/{}^{234}\text{Th}_{\text{ex}}$ inventory ratios,
525 ranging from 0.16 to 0.95, displays a significant difference ($p < 0.05$) with the values
526 obtained at a larger distance. These correspond to the continental shelf (distance from the
527 river mouth $> 8.5 \text{ km}$), with stations D, E, R and U designated as Zone III (surface area
528 off river mouth $> 150 \text{ km}^2$), with ${}^7\text{Be}/{}^{234}\text{Th}_{\text{ex}}$ inventory ratios ranging from 0.02 to 0.07.
529 This indicates that the inputs of river-borne particles are dominant in zone I, while zone
530 III is characterized by a stronger marine particle influence. At an intermediate distance
531 (i.e., distance from the river mouth = 3.0-8.5 km) with Stns. AZ, B, C, G, K, L, N, and O
532 (defined as Zone II), the ${}^7\text{Be}/{}^{234}\text{Th}_{\text{ex}}$ inventory ratios are between 0.05 and 0.30
533 suggesting a mixed influence of particles labelled by river and seawater, recently
534 deposited in this area. The zoning based on inventory ratios is presented in Figure 9 and
535 summarized in Table 3. This zoning is comparable to the observation by Rassmann et al.
536 (2016), who demonstrated that the average oxygen penetration depth into Zone I
537 sediment was one fifth of that in Zone III. In addition, Zone I, which corresponds mainly
538 to the pro-deltaic area, appears to be the area where most of the particle associated
539 contaminants driven by the Rhône River into the Gulf of Lions are deposited (Miralles et

540 al., 2004; Roussiez et al., 2005). This zoning is therefore helpful for further understanding
541 the spreading of particles-associated contaminants, such as man-made radionuclides and
542 heavy metals, in the Gulf of Lions (Charmasson et al., 1998; Radakovitch et al., 2008;
543 Ferrand et al., 2012) and its initial sedimentary deposition in the Gulf of Lions. This study
544 provides an effective reference to assess riverine and marine influence beyond the Rhône,
545 which is very important for understanding the initial deposition of riverine particles as
546 tracking the recent particles deposition on the time scale of a few months has been rarely
547 performed in deltas and estuaries.

548

549 **5. Conclusions**

550 Short-term deposition of particles close to the Rhône River mouth in the Gulf of
551 Lions was traced by natural radionuclides ^7Be and $^{234}\text{Th}_{\text{ex}}$. Both the ^7Be and $^{234}\text{Th}_{\text{ex}}$
552 inventories are larger at the Rhône River mouth and were correlated with cumulated SPM
553 fluxes calculated over two half-lives before the sampling date. The spatial distributions of
554 ^7Be inventories and $^7\text{Be}/^{234}\text{Th}_{\text{ex}}$ inventory ratios showed an exponential decrease with
555 distance from the river mouth. Their distributions indicated that recent particles are
556 mainly deposited within a ~ 5 km radius from the river mouth and that maximal
557 deposition occurs within 3 km off the river mouth. These areas of recently deposited
558 particles coincide with areas with high apparent accumulation rates determined over
559 longer time scale using longer half-life radionuclides such as ^{137}Cs (ref?). Moreover, the
560 gradients in sediment $^7\text{Be}/^{234}\text{Th}_{\text{ex}}$ inventory ratio observed in the studied area lend
561 support to the notion that this ratio can be used as a potential index for identifying the
562 dominant influence between the river and the sea on the deposited particles, which is
563 really driven by ^7Be in this study. The riverine and marine influences can be classified as
564 follows: Zone I (distance from the river mouth < 3.0 km with $^7\text{Be}/^{234}\text{Th}_{\text{ex}}$ inventory ratio
565 over 0.50, surface area near river mouth ~ 7 km²) is dominated by riverine input, while
566 Zone III (distance from the river mouth beyond 8.5 km with $^7\text{Be}/^{234}\text{Th}_{\text{ex}}$ inventory ratio
567 less than 0.10, surface area off river mouth beyond 150 km²) is predominantly under a
568 marine influence. In between, the transition zone displays a mixed influence, (transition
569 Zone II, distance from the river mouth: 3.0-8.5 km with $^7\text{Be}/^{234}\text{Th}_{\text{ex}}$ inventory ratios
570 between 0.10 and 0.50).

Commenté [s7]: no need to repeat

571

572

573 **Author information**

574 * **Corresponding authors:**

575 Tel: +33-4-94-30-48-29, Fax: +33-4-94-30-44-16 (S. Charmasson).

576 E-mail: christophe.rabouille@lsce.ipsl.fr (C. Rabouille).

577 sabine.charmasson@irsn.fr (S. Charmasson).

Code de champ modifié

Code de champ modifié

578 **Notes**

579 The authors declare that there is no competing financial interest.

580 **Author Contributions**

581 The manuscript was written through contributions from all authors. All authors have
582 given approval to the final version of the manuscript.

583

584 **Acknowledgements**

585 This work was supported by the AMORAD project (French state financial support
586 managed by the National Agency for Research allocated in the “Investments for the
587 Future” framework program under reference ANR-11-RSNR-0002), and funding project
588 for scientific research startup of Shantou University. Funding was also provided by the
589 Midi Pyrénées-Paca Interregional Project CARMA, ANR-EXTREMA, ANR-CHACCRA
590 the EC2CO Riomar.fr, and Mistrals/Mermex through the “Mermex-Rivers” action. We
591 thank the captains and crews of the R.V. Europe and Tethys II for their collaboration
592 during the sampling expeditions. We deeply thank Mireille Arnaud, chief scientist of the
593 CARMEX (March 2007) and Extrema1 (March 2008) cruises. We are very grateful to
594 *Compagnie Nationale du Rhône* and *MOOSE/SORA observatory* in Arles for providing
595 freshwater discharge and particle load data, respectively.

596

597 **References**

598 Aller, R.C., Cochran, J.K., 1976. $^{234}\text{Th}/^{238}\text{U}$ disequilibrium in near-shore sediment:
599 particle reworking and diagenetic time scales. *Earth Planet. Sci. Lett.* 29, 37-50.

600 Alliot, E., Younes, W.A., Romano, J.C., Rebouillon, P., Masse, H., 2003. Biogeochemical

601 impact of a dilution plume (Rhône River) on coastal sediments: comparison between a
602 surface water survey (1996-2000) and sediment composition. *Estuar. Coast. Shelf Sci.*
603 *57*, 357-367.

604 Aloisi, J.C., Millot, C., Monaco, A., Pauc, H., 1979. Dynamique des suspensions et
605 mecanismes sedimentologiques sur le plateau continental du Golfe du Lion. *C.R. Acad.*
606 *Sci. Paris D 289*, 879-882.

607 Antonelli, C., 2002. Flux sedimentaires et morphogenese recente dans le chenal du Rhône
608 aval. Universite de Provence, Aix en Provence, pp 272.

609 Antonelli, C., Eyrolle, F., Rolland, B., Provansal, M., Sabatier, F., 2008. Suspended
610 sediment and ^{137}Cs fluxes during the exceptional December 2003 flood in the Rhône
611 River, southeast France. *Geomorphology* *95*, 350-360.

612 Arnoux-Chiavassa, S., Rey, V., Fraunie, P., 2003. Modeling 3D Rhône River plume using
613 a higher order advection scheme. *Oceanol. Acta* *26*, 299-309.

614 Baskaran, M., Ravichandran, M., Bianchi, T.S., 1997. Cycling of ^7Be and ^{210}Pb in a high
615 DOC shallow, turbid estuary of south-east Texas. *Estuar. Coast. Shelf Sci.* *45*, 165-176.

616 Baskaran, M., Swarzenski, P.W., 2007. Seasonal variations on the residence times and
617 partitioning of short-lived radionuclides (^{234}Th , ^7Be and ^{210}Pb) and depositional fluxes
618 of ^7Be and ^{210}Pb in Tampa Bay, Florida. *Mar. Chem.* *104*, 27-42.

619 Bianchi, T.S., Allison, M.A., 2009. Large-river delta-front estuaries as natural “recorders”
620 of global environmental change. *Proc. Nat. Acad. Sci.* *106*, 8085-8092.

621 Bonifacio, P., Bourgeois, S., Labrune, C., Amourous, J.M., Escoubeyrou, K., Buscail, R.,
622 Romero-Ramirez, A., Lantoine, F., Vetion, G., Bichon, S., Desmalades, M., Riviere, B.,
623 Deflandre, B., Gremare, A., 2014. Spatiotemporal changes in surface sediment
624 characteristics and benthic macrofauna composition off the Rhône River in relation to
625 its hydrological regime. *Estuar. Coast. Shelf Sci.* *151*, 196-209.

626 Bourgeois, S., Pruski, A.M., Sun, M.Y., Buscail, R., Lantoine, F., Kerherve, P., Vetion, G.,
627 Riviere, B., Charles, F., 2011. Distribution and lability of land-derived organic matter
628 in the surface sediments of the Rhône prodelta and the adjacent shelf (Mediterranean
629 Sea, France): a multi proxy study. *Biogeosciences* *8*, 3107-3125.

630 Cai, W.J., 2011. Estuarine and coastal ocean carbon paradox: CO_2 sinks or sites of
631 terrestrial carbon incineration. *Ann. Rev. Mar. Sci.* *3*, 123-145.

632 Calmet, D., Fernandez, J.M., 1990. Caesium distribution in northwest Mediterranean
633 seawater, suspended particles and sediments. *Cont. Shelf Res.* 10, 895-913.

634 Cathalot, C., Rabouille, C., Pastor, L., Deflandre, B., Viollier, E., Buscail, R., Gremare, A.,
635 Treignier, C., Pruski, A., 2010. Temporal variability of carbon recycling in coastal
636 sediments influenced by rivers: assessing the impact of flood inputs in the Rhône River
637 prodelta. *Biogeosciences* 7, 1187-1205.

638 Cathalot, C., Rabouille, C., Tisnerat-Laborde, N., Toussaint, F., Kerherve, P., Buscail, R.,
639 Loftis, K., Sun, M.Y., Tronczynski, J., Azoury, S., Lansard, B., Treignier, C., Pastor, L.,
640 Tesi, T., 2013. The fate of river organic carbon in coastal areas: a study in the Rhône
641 River delta using multiple isotopic ($\delta^{13}\text{C}$, $\Delta^{14}\text{C}$) and organic tracers. *Geochim.*
642 *Cosmochim. Acta* 118, 33-55.

643 Cazala, C., Reyss, J.L., Decossas, J.L., Royer, A., 2003. Improvement in the
644 determination of ^{238}U , $^{228-234}\text{Th}$, $^{226-228}\text{Ra}$, ^{210}Pb and ^7Be by spectrometry on evaporated
645 fresh water samples. *Environ.Sci. Technol.* 37, 4990-4993.

646 Charmasson, S., 2003. ^{137}Cs inventory in sediment near the Rhône mouth: role played by
647 different sources. *Oceanol. Acta* 26, 435-441.

648 Charmasson, S., Bouisset, P., Radakovitch, O., Pruchon, A.S., Amaud, M., 1998.
649 Long-core profiles of ^{137}Cs , ^{134}Cs , ^{60}Co and ^{210}Pb in sediment near the Rhône River
650 (Northwestern Mediterranean Sea). *Estuaries* 21, 367-378.

651 Chen, C.T.A., Borges, A.V., 2009. Continental shelves as sinks and near-shore
652 ecosystems as sources of atmospheric CO_2 . *Deep-Sea Res.* 56, 578-590.

653 Corbett, D.R., Dail, M., McKee, B., 2007. High-frequency time-series of the dynamic
654 sedimentation processes on the western shelf of the Mississippi River deltaic. *Cont.*
655 *Shelf Res.* 27, 1600-1615.

656 Corbett, D.R., McKee, B., Duncan, D., 2004. An evaluation of mobile mud dynamics in
657 the Mississippi River deltaic region. *Mar. Geol.* 209, 91-112.

658 Cutshall, N.H., Larsen, I.L., Olsen, C.R., 1983. Direct analysis of ^{210}Pb in sediment
659 samples: self-adsorption corrections. *Nucl. Instrum. Methods* 206, 309-312.

660 Dagg, M., Benner, R., Lohrenz, S., Lawrence, D., 2004. Transformation of dissolved and
661 particulate materials on continental shelves influenced by large rivers: plume processes.
662 *Cont. Shelf Res.* 24, 833-858.

663 De Madron, X.D., Abassi, A., Heussner, S., Monaco, A., Aloisi, J.C., Radakovitch, O.,
664 Giresse, P., Buscail, R., Kerherve, P., 2000. Particulate matter and organic carbon
665 budgets for the Gulf of Lions (NW Mediterranean). *Oceanol. Acta* 23, 717-730.
666 De Vismes Ott, A., Gurriaran, R., Cagnat, X., Masson, O., 2013. Fission product activity
667 ratios measured at trace level over France during the Fukushima accident. *J. Environ.*
668 *Radioact.* 125, 6-16.
669 Delanghe, D., Bard, E., Hamelin, B., 2002. New TIMS constraints on the uranium-238
670 and uranium-234 in seawaters from the main ocean basins and the Mediterranean Sea.
671 *Mar. Chem.* 80, 79-93.
672 Dobb, J.E., Rice, D.L., 1989. The geochemistry of beryllium-7 in Chesapeake Bay. *Estuar.*
673 *Coast. Shelf Sci.* 28, 379-394.
674 Drexler, T.M., Nittrouer, C.A., 2008. Stratigraphic signatures due to flood deposition near
675 the Rhône River: Gulf of Lions, northwest Mediterranean Sea. *Cont. Shelf Res.* 28,
676 1877-1894.
677 Dufois, F., Garreau, P., Le Hir, P., Forget, P., 2008. Wave- and current-induced bottom
678 shear stress distribution in the Gulf of Lions. *Cont. Shelf Res.* 28, 1920-1934.
679 Dufois, F., Verney, R., Le Hir, P., Dumas, F., Charmasson, S., 2014. Impact of winter
680 storms on sediment erosion in the Rhône River prodelta and fate of sediment in the
681 Gulf of Lions (North Western Mediterranean Sea). *Cont. Shelf Res.* 72, 57-72.
682 Durrieu de Madron, X., Abassi, A., Heussner, S., Monaco, A., Aloisi, J.C., Radakovitch,
683 O., Giresse, P., Buscail, R., Kerherve, P., 2000. Particulate matter and organic carbon
684 budgets for the Gulf of Lions (NW Mediterranean). *Oceanol. Acta* 23, 717-730.
685 Eyrolle, F., Charmasson, S., Louvat, D., 2004. Plutonium isotopes in the lower reaches of
686 the river Rhône over the period 1945-2000: fluxes towards the Mediterranean Sea and
687 sedimentary inventories. *J. Environ. Radioact.* 74, 127-138.
688 Eyrolle, F., Radakovitch, O., Raimbault, P., Charmasson, S., Antonelli, C., Ferrand, E.,
689 Aubert, D., Raccasi, G., Jacquet, S., Gurriaran, R., 2012. Consequences of
690 hydrological events on the delivery of suspended sediment and associated
691 radionuclides from the Rhône River to the Mediterranean Sea. *J. Soils Sediment* 12,
692 1479-1495.
693 Fanget, A.S., Bassetti, M.A., Arnaud, M., Chiffolleau, J.F., Cossa, D., Goineau, A.,

694 Fontanier, C., Buscail, R., Jouet, G., Maillet, G. M., Negri, A., Dennielou, B., Berne, S.,
695 2013. Historical evolution and extreme climate events during the last 400 years on the
696 Rhône prodelta (NW Mediterranean). *Mar. Geol.* 346, 375-391.

697 Fay, M.P., Proschan, M.A., 2010. Wilcoxon-Mann-Whitney or t-test? On assumptions for
698 hypothesis tests and multiple interpretations of decision rules. *Stat. Surv.* 4, 1-39.

699 Feng, H., Cochran, J. K., Hirschberg, D.J., 1999a. ^{234}Th and ^7Be as tracers for transport
700 and dynamics of suspended particles in a partially mixed estuary. *Geochim.*
701 *Cosmochim. Acta* 63, 2487-2505.

702 Feng, H., Cochran, J.K., Hirschberg, D.J., 1999b. ^{234}Th and ^7Be as tracers for transport
703 and sources of particle-associated contaminants in the Hudson River Estuary. *Sci. Total*
704 *Environ.* 237/238, 401-418.

705 Ferrand, E., Eyrolle, F., Radakovitch, O., Provansal, M., Dufour, S., Vella, C., Raccasi, G.,
706 Gurriaran, R., 2012. Historical levels of heavy metals and artificial radionuclides
707 reconstructed from overbank sediment records in lower Rhône River (South-East
708 France). *Geochim. Cosmochim. Acta* 82, 163-182.

709 Fitzgerald, S.A., Klump, J.V., Swarzenski, P.W., Mackenzie, R.A., Richards, K.D., 2001.
710 Beryllium-7 as a tracer of short-term sediment deposition and resuspension in the Fox
711 River, Wisconsin. *Environ. Sci. Technol.* 35, 300-305.

712 Got, H., Aloisi, J.C., 1990. The Holocene sedimentation on the Gulf of Lions margin: a
713 quantitative approach. *Cont. Shelf Res.* 10, 841-855.

714 Guo, L.D., Santschi, P.H., Baskaran, H., Zindler, A., 1995. Distribution of dissolved and
715 particulate ^{230}Th and ^{232}Th in seawater from the Gulf of Mexico and off Cape Hatteras
716 as measured by SIMS. *Earth Planet. Sci. Lett.* 133, 117-128.

717 IAEA, 2004. Sediment distribution coefficients and concentration factors for biota in the
718 marine environment. Technical Reports Series 422, IAEA, Vienna, pp 95.

719 Ibanez, C., Pont, D., Prat, N., 1997. Characterization of the Ebre and Rhône estuaries: a
720 basis for defining and classifying salt-wedge estuaries. *Limnol. Oceanogr.* 42, 89-101.

721 Ku, T.L., Knauss, K.G., Mathieu, G.G., 1977. Uranium in open ocean: concentration and
722 isotopic composition. *Deep-Sea Res.* 24, 1005-1017.

723 Lal, D., Malhotra, P.K., Peters, B., 1958. On the production of radioisotopes in the
724 atmosphere by cosmic radiation and their application to meteorology. *J. Atoms. Terr.*

725 Phys. 12, 306-328.

726 Lansard, B., Charmasson, S., Gasco, C., Anton, M.P., Grenz, C., Arnaud, M., 2007.

727 Spatial and temporal variations of plutonium isotopes (^{238}Pu and $^{239,240}\text{Pu}$) in sediments

728 off the Rhône River mouth (NW Mediterranean). *Sci. Total Environ.* 376, 215-227.

729 Lansard, B., Rabouille, C., Denis, L., Grenz, C., 2009. Benthic remineralization at the

730 land-ocean interface: a case study of the Rhône River (NW Mediterranean Sea). *Estuar.*

731 *Coast. Shelf Sci.* 81, 544-554.

732 Larsen, I.L., Cutshall, N.H., 1981. Direct determination of ^7Be in sediments. *Earth Planet.*

733 *Sci. Lett.* 54, 379-384.

734 Lefevre, O., Bouisset, P., Germain, P., Barker, E., Kerlau, G., Cagnat, X., 2003.

735 Self-absorption correction factor applied to ^{129}I measurement by direct gamma-X

736 spectrometry for *Fucus serratus* samples. *Nucl. Instr. Meth. Phys. Res. A* 506, 173-185.

737 Maillet, G.M., Vella, C., Berne, S., Friend, P.L., Amos, C.L., Fleury, T.J., Normand, A.,

738 2006. Morphological changes and sedimentary processes induced by the December

739 2003 flood event at the present mouth of the Grand Rhône River (southern France).

740 *Mar. Geol.* 234, 159-177.

741 Mangini, A., Sonntag, C., Bertsch, G., Muller, E., 1979. Evidence for a high natural

742 uranium content in world rivers. *Nature* 278, 337-339.

743 Many, G., Bourrin, F., Durrieu de Madron, X., Pairaud, I., Gangloff, A., Doxaran, D., Ody,

744 A., Verney, R., Menniti, C., Le Berre, D., Jacquet, M., 2016. Particle assemblage

745 characterization in the Rhône River ROFI. *J. Mar. Syst.* 157, 39-51.

746 Many, G., Bourrin, F., Durrieu de Madron, X., Ody, A., Doxaran, D., 2018. Glider and

747 satellite monitoring of the variability of the suspended particle distribution and size in

748 the Rhône ROFI. *Progr. Oceano*, 163, 123-135.

749 Marion, C., Dufois, F., Arnaud, M., Vella, C., 2010. In situ record of sedimentary

750 processes near the Rhône River mouth during winter events (Gulf of Lions,

751 Mediterranean Sea). *Cont. Shelf Res.* 30, 1095-1107.

752 Matisoff, G., Bonniwell, E.C., Whiting, P.J., 2002. Soil erosion and sediment sources in

753 an Ohio watershed using beryllium-7, cesium-137, and lead-210. *J. Environ. Qual.* 31,

754 54-61.

755 McCubbin, D., Leonard, K.S., Greenwood, R.C., Taylor, B.R., 2004. Solid-solution

756 partitioning of plutonium in surface waters at the Atomic Weapons Establishment
757 Aldermaston (UK). *Sci. Total Environ.* 332, 203-216.

758 McKee, B.A., Aller, R.C., Allison, M.A., Bianchi, T.S., Kineke, G.C., 2004. Transport
759 and transformation of dissolved and particulate materials on continental margins
760 influenced by major rivers: benthic boundary layer and seabed processes. *Cont. Shelf*
761 *Res.* 24, 899-926.

762 Milliams, J., Rose, C.P., 2001. Measured and predicted rates of sediment transport in
763 storm conditions. *Mar. Geol.* 179, 121-133.

764 Miralles, J., Arnaud, M., Radakovitch, O., Marion, C., Cagnat, X., 2006. Radionuclide
765 deposition in the Rhône River Prodelta (NW Mediterranean Sea) in response to the
766 December 2003 extreme flood. *Mar. Geol.* 234, 179-189.

767 Miralles, J., Radakovitch, O., Aloisi, J.C., 2005. ²¹⁰Pb sedimentation rates from the
768 Northwestern Mediterranean margin. *Mar. Geol.* 216, 155-167.

769 Miralles, J., Radakovitch, O., Cochran, J.K., Veron, A., Masque, P., 2004. Multitracer
770 study of anthropogenic contamination records in the Camargue, Southern France. *Sci.*
771 *Total Environ.* 320, 63-72.

772 Moore, W.S., de Oliveira, J., 2008. Determination of residence time and mixing processes
773 of the Ubatuba, Brazil, inner shelf waters using natural Ra isotopes. *Estuar. Coast.*
774 *Shelf Sci.* 76, 512-521.

775 Mullenbach, B.L., Nittrouer, C.A., Puig, P., Orange, D.L., 2004. Sediment deposition in a
776 modern submarine canyon: Eel Canyon, Northern California. *Mar. Geol.* 211, 101-119.

777 Naudin, J.J., Cauwet, G., Chretiennot-Dinet, M.J., Deniaux, B., Devenon, J.L., Pauc, H.,
778 1997. River discharge and wind influence upon particulate transfer at the land-ocean
779 interaction: case study of the Rhône River plume. *Estuar. Coast. Shelf Sci.* 45,
780 303-316.

781 Ogston, A.S., Drexler, T.M., Puig, P., 2008. Sediment delivery, resuspension, and
782 transport in two contrasting canyon environments in the southwest Gulf of Lions. *Cont.*
783 *Shelf Res.* 28, 2000-2016.

784 Ollivier, P., Radakovitch, O., Hamelin, B., 2011. Major and trace element partition and
785 fluxes in the Rhône River. *Chem. Geol.* 285, 15-31.

786 Olsen, C.R., Larsen, I.L., Lowry, P.D., Cutshall, N.H., Nichols, M.M., 1986.

787 Geochemistry and deposition of ^7Be in river-estuarine and coastal water. *J. Geophys.*
788 *Res.* 91, 896-908.

789 Owens, S.A., Buesseler, K.O., Sims, K.W.W., 2012. Re-evaluating the ^{238}U -salinity
790 relationship in seawater: implications for the ^{238}U - ^{234}Th disequilibrium method. *Mar.*
791 *Chem.* 127, 31-39.

792 Palinkas, C.M., Nittrouer, C.A., Wheatcroft, R.A., Langone, L., 2005. The use of ^7Be to
793 identify event and seasonal sedimentation near the Po River delta, Adriatic Sea. *Mar.*
794 *Geol.* 222/223, 95-112.

795 Pastor, L., Deflandre, B., Viollier, E., Cathalot, C., Metzger, E., Rabouille, C.,
796 Escoubeyrou, K., Lloret, E., Pruski, A.M., Vétion, G., Desmalades, M., Buscail, R.,
797 Gremare, A., 2011. Influence of the organic matter composition on benthic oxygen
798 demand in the Rhône River prodelta (NW Mediterranean Sea). *Cont. Shelf Res.* 31,
799 1008-1019.

800 Perianez, R., 2005. Modelling the transport of suspended particulate matter by the Rhône
801 River plume (France). Implications for pollutant dispersion. *Environ. Pollut.* 133,
802 351-364.

803 Pont, D., Simonnet, J.P., Walter, A.V., 2002. Medium-term changes in suspended
804 sediment delivery to the ocean: consequences of catchment heterogeneity and river
805 management (Rhône River, France). *Estuar. Coast. Shelf Sci.* 54, 1-18.

806 Radakovitch, O., Charmasson, S., Arnaud, M., Bouisset, P., 1999. ^{210}Pb and caesium
807 accumulation in the Rhône delta sediment. *Estuar. Coast. Shelf Sci.* 48, 77-99.

808 Radakovitch, O., Roussiez, V., Ollivier, P., Ludwig, W., Grenz, C., Probst, J.L., 2008.
809 Input of particulate heavy metals from rivers and associated sedimentary deposits on
810 the Gulf of Lion continental shelf. *Estuar. Coast. Shelf Sci.* 77, 285-295.

811 Rassmann, J., Lansard, B., Pozzato, L., Rabouille, C., 2016. Carbonate chemistry in
812 sediment porewaters of the Rhône River delta driven by early diagenesis (northwestern
813 Mediterranean). *Biogeosciences* 13, 5379-5394.

814 Reyss, J.L., Schmidt, S., Legeleux, F., Bonté, P., 1995. Large, low background well type
815 detectors for the measurement of environmental radioactivity. *Nucl. Instrum. Methods*
816 *Physic. Res. Sec A* 357, 391-397.

817 Roussiez, V., Aloisi, J.C., Monaco, A., Ludwig, W., 2005. Early muddy deposits along the

818 Gulf of Lions shoreline: A key for a better understanding of land-to-sea transfer of
819 sediments and associated pollutant fluxes. *Mar. Geol.* 222-223, 345-358.

820 Roussiez, V., Ludwig, W., Monaco, A., Probst, J.L., Bouloubassi, I., Buscail, R., Saragoni,
821 G., 2006. Sources and sinks of sediment-bound contaminants in the Gulf of Lions (NW
822 Mediterranean Sea): a multi-tracer approach. *Cont. Shelf Res.* 26, 1843-1857.

823 Saari, H.K., Schmidt, S., Castaing, P., Blanc, G., Sautour, B., Masson, O., Cochran, J.K.,
824 2010. The particulate ${}^7\text{Be}/{}^{210}\text{Pb}_{\text{xs}}$ and ${}^{234}\text{Th}/{}^{210}\text{Pb}_{\text{xs}}$ activity ratios as tracers for
825 tidal-to-seasonal particle dynamics in the Gironde estuary (France): Implications for
826 the budget of particle-associated contaminants. *Sci. Total Environ.* 408, 4784-4794.

827 Sadaoui, M., Ludwig, W., Bourrin, F., Raimbault, P., 2016. Controls, budgets and
828 variability of riverine sediment fluxes to the Gulf of Lions (NW Mediterranean Sea). *J.*
829 *Hydrol.* 540, 1002-1015.

830 Sanford, L.P., 1992. New sedimentation, resuspension, and burial. *Limnol. Oceanogr.* 37,
831 1164-1178.

832 Santschi, P.H., Guo, L., Walsh, I.D., Quigley, M.S., Baskaran, M., 1999. Boundary
833 exchange and scavenging of radionuclides in continental margin waters of the Middle
834 Atlantic Bight: implications for organic carbon fluxes. *Cont. Shelf Res.* 19, 609-636.

835 Sempéré, R., Charriere, B., Van Wambeke, F., Cauwet, G., 2000. Carbon inputs of the
836 Rhône River to the Mediterranean Sea: biogeochemical implications. *Glob.*
837 *Biogeochem. Cy.* 14, 669-681.

838 Skwarzec, B., 1995. Polonium, uranium and plutonium in southern Baltic ecosystem.
839 Thesis and monographies, Institute of Oceanology PAN, 6, Sopot.

840 Sommerfield, C.K., Nittrouer, C.A., Alexander, C.R., 1999. ${}^7\text{Be}$ as a tracer of flood
841 sedimentation on the northern California continental margin. *Cont. Shelf Res.* 19,
842 335-361.

843 Su, N., Du, J., Moore, W.S., Liu, S., Zhang, J., 2011. An examination of groundwater
844 discharge and the associated nutrient fluxes into the estuaries of eastern Hainan Island,
845 China using ${}^{226}\text{Ra}$. *Sci. Total Environ.* 409, 3909-3918.

846 Syvitski, J.P.M., Saito, Y., 2007. Morphodynamics of deltas under the influence of
847 humans. *Glob. Planet. Change* 57, 261-282.

848 Taylor, A., Blake, W.H., Smith, H.G., Mabit, L., Keith-Roach, M.J., 2013. Assumptions

849 and challenges in the use of fallout beryllium-7 as a soil and sediment tracer in river
850 basins. *Earth Sci. Rev.* 126, 85-95.

851 Thill, A., Moustier, S., Garnier, J.M., Estournel, C., Naudin, J.J., Bottero, J.Y., 2001.
852 Evolution of particle size and concentration in the Rhône River mixing zone: influence
853 of salt flocculation. *Cont. Shelf Res.* 21, 2127-2140.

854 Ulses, C., Estournel, C., Durrieu de Madron, X., Palanques, A., 2008. Suspended
855 sediment transport in the Gulf of Lions (NW Mediterranean): impact of extreme storms
856 and floods. *Cont. Shelf Res.* 28, 2048-2070.

857 Wallbrink, P.J., Murray, A.S., 1994. Fallout of ^7Be in south Eastern Australia. *J. Environ.*
858 *Radioact.* 25, 213-228.

859 Wallbrink, P.J., Murray, A.S., 1996. Distribution and variability of ^7Be in soils under
860 different surface cover conditions and its potential for describing soil redistribution
861 processes. *Water Resour. Res.* 32, 467-476.

862 Wang, J.L., Du, J.Z., Baskaran, M., Zhang, J., 2016. Mobile mud dynamics in the East
863 China Sea elucidated using ^{210}Pb , ^{137}Cs , ^7Be , and ^{234}Th as tracers. *J. Geophys. Res.*
864 *Oceans* 121, 224-239.

865 Wang, Z.L., Yamada, M., 2005. Plutonium activities and $^{240}\text{Pu}/^{239}\text{Pu}$ atom ratios in
866 sediment cores from the East China Sea and Okinawa Trough: sources and inventories.
867 *Earth Planet. Sci. Lett.* 233, 441-453.

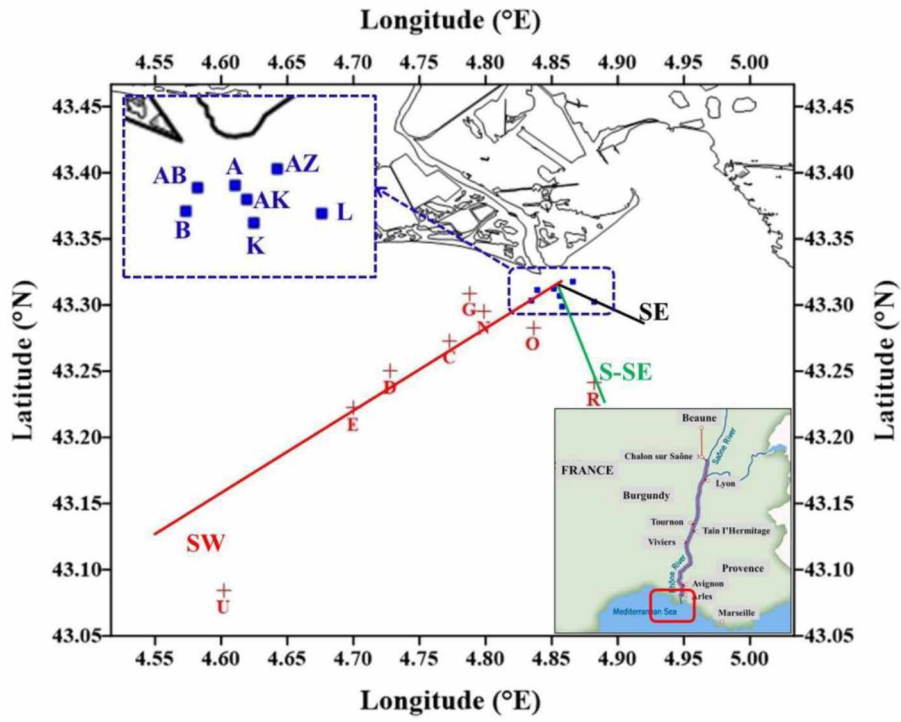
868 Yeager, K.M., Santschi, P.H., Rowe, G.T., 2004. Sediment accumulation and radionuclide
869 inventories (Pu-239, Pu-240, Pu-210 and Th-234) in the northern Gulf of Mexico, as
870 influenced by organic matter and macrofaunal density. *Mar. Chem.* 91, 1-14.

871 Zebracki, M., Cagnat, X., Gairoard, S., Cariou, N., Eyrolle, F., Boulet, B., Antonelli, C.,
872 2017. U isotopes distribution in the lower Rhône River and its implication on
873 radionuclides disequilibrium within the decay series. *J. Environ. Radioact.* 178-179,
874 279-289.

875 Zebracki, M., Eyrolle, F., Evrard, O., Claval, D., Mourier, B., Gairoard, S., Cagnat, X.,
876 Antonelli, C., 2015. Tracing the origin of suspended sediment in a large Mediterranean
877 river by combining continuous river monitoring and measurement of artificial and
878 natural radionuclides. *Sci. Total Environ.* 502, 122-132.

879

880



881

882

Figure 1. Maps of the Rhône River pro-delta showing the sampling locations.

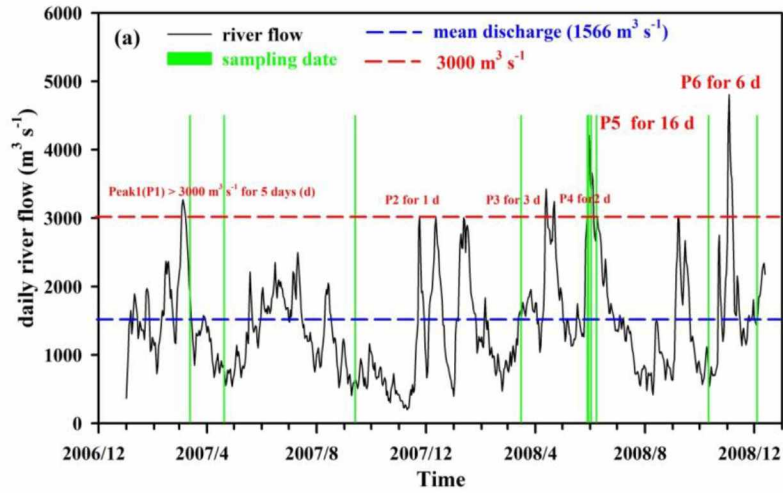
883

884

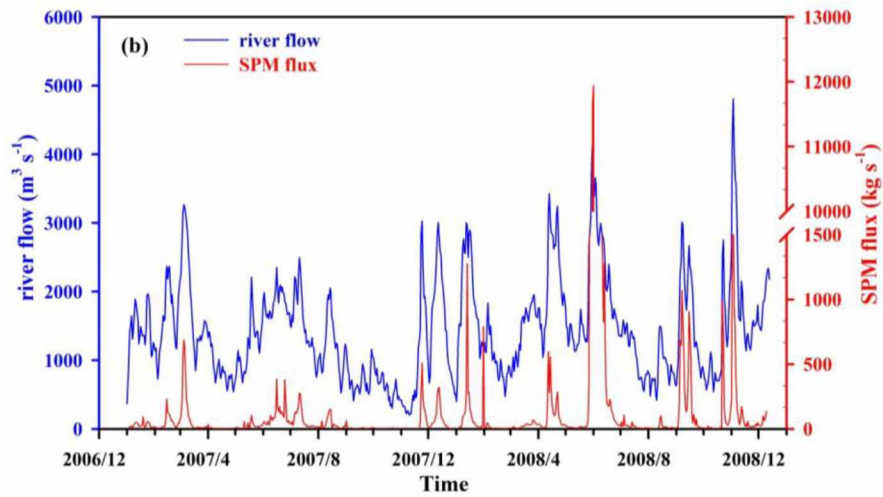
885

886

887



888



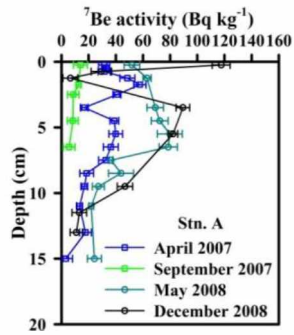
889

890 **Figure 2.** The daily variation of the Rhône River flow (a) and the relationship between
 891 river flow and Suspended Particulate Matter (SPM) fluxes (b) during the period of
 892 2007-2008.

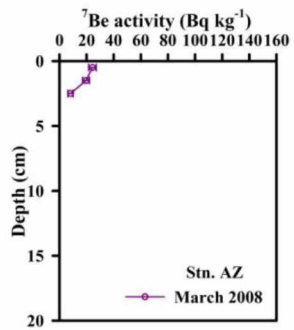
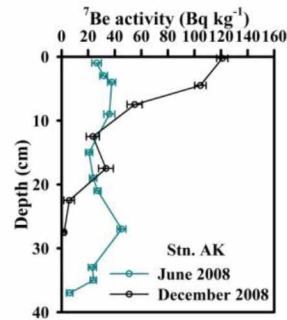
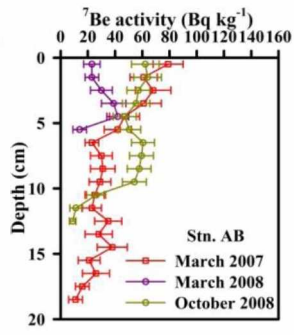
893

894

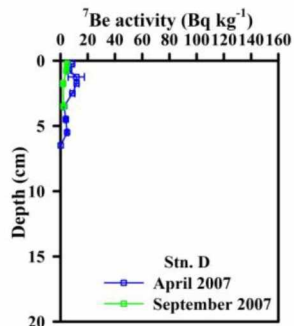
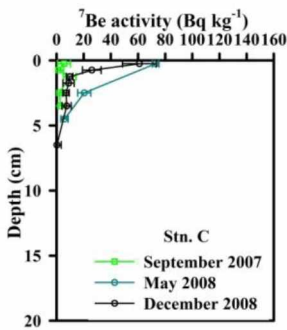
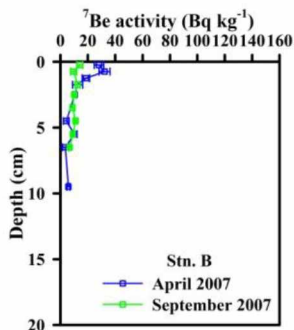
895



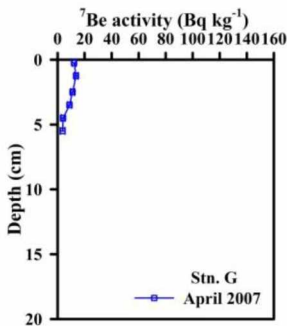
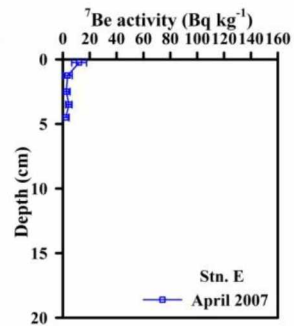
896

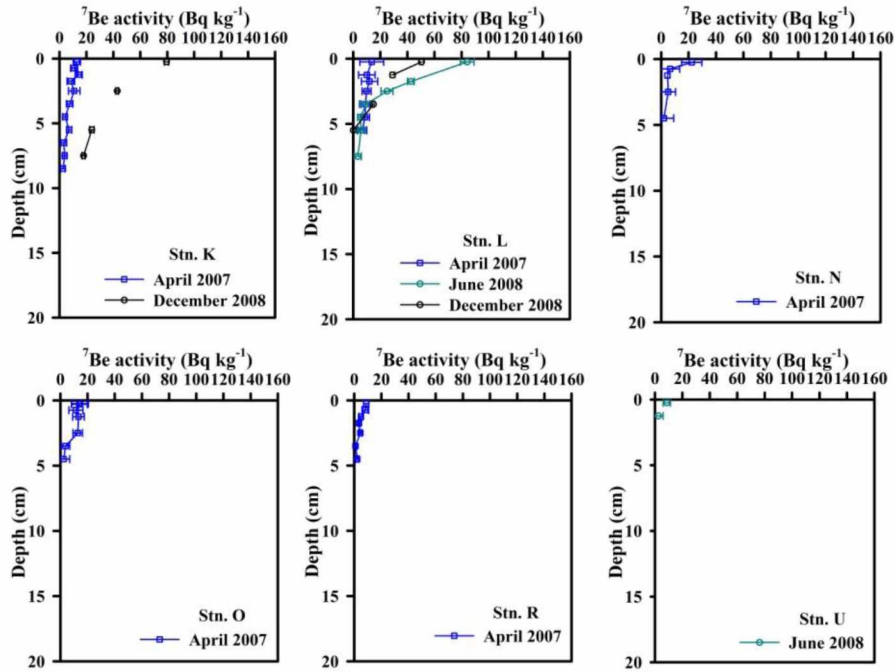


897



898





899

900

901

902

Figure 3. Vertical distributions of ^7Be activities in the sediment cores.

903

904

905

906

907

908

909

910

911

912

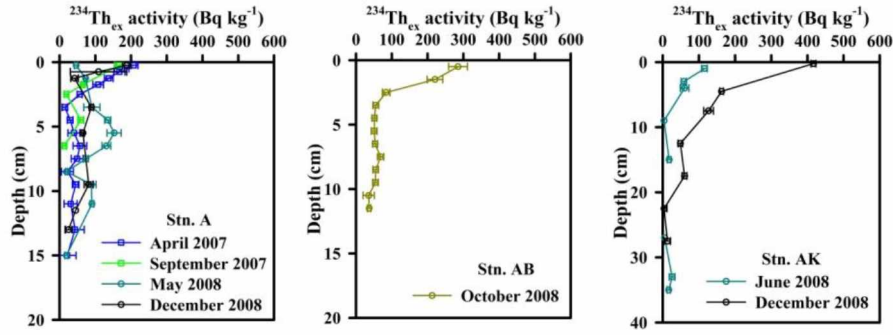
913

914

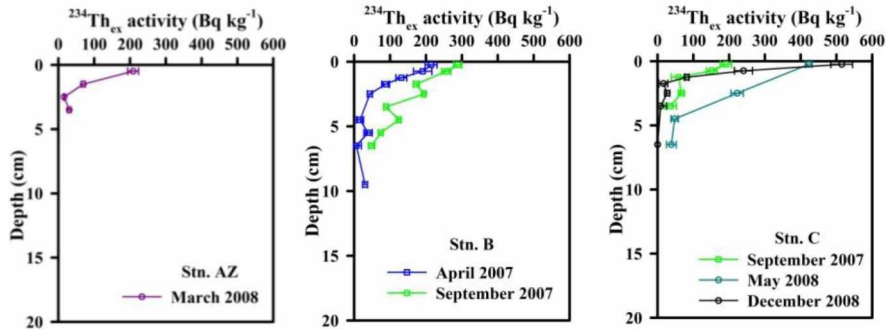
915

916

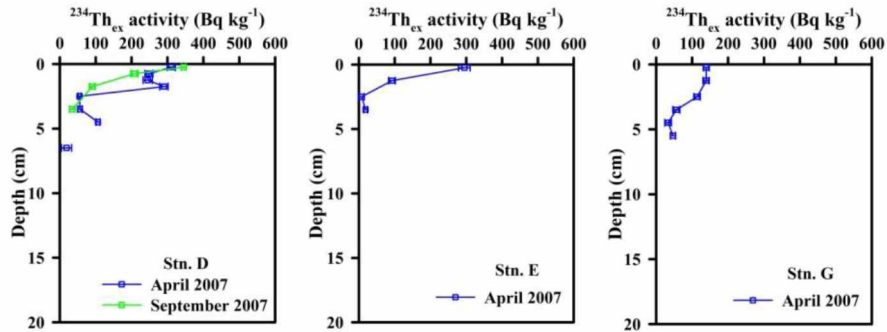
917



918



919



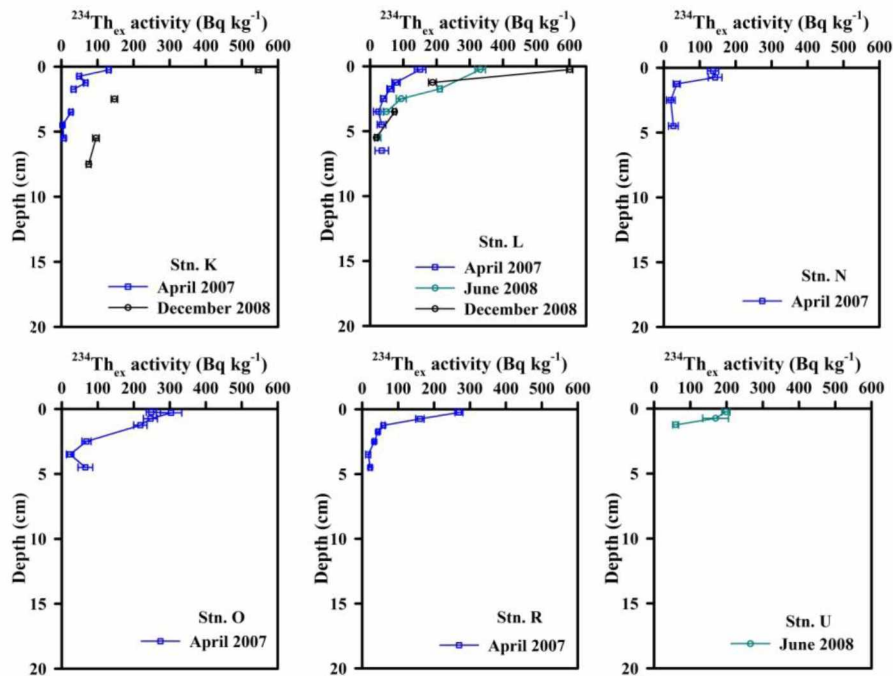


Figure 4. Vertical distributions of $^{234}\text{Th}_{\text{ex}}$ activities in the sediment cores.

920

921

922

923

924

925

926

927

928

929

930

931

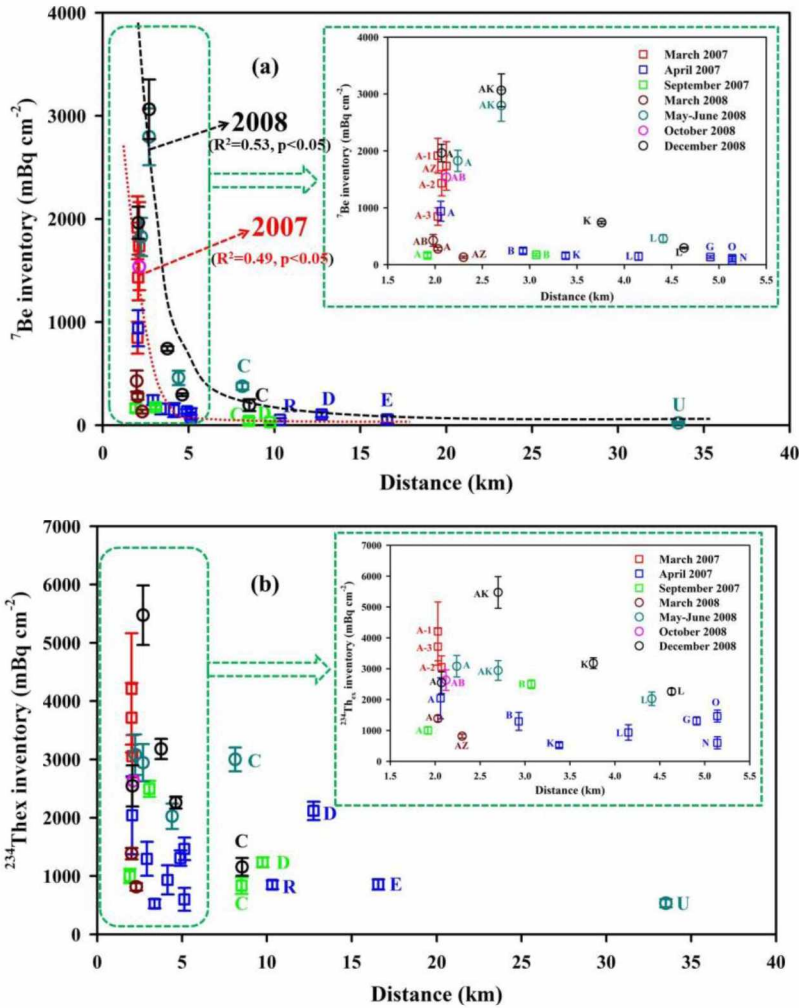
932

933

934

935

936



937

938

939

940

941

942

943

944

945

Figure 5. Inventories of ${}^7\text{Be}$ (a) and ${}^{234}\text{Th}_{\text{ex}}$ (b) in the sediment cores, as a function of distance off the Rhône River mouth for March 2007 (red empty squares), April 2007 (blue empty squares), September 2007 (green empty squares), March 2008 (dark red empty circles), May-June 2008 (dark cyan empty circles), October 2008 (purple empty circles) and December 2008 (black empty circles). The exponential decreases of the ${}^7\text{Be}$ inventories with distance in 2007 and 2008 are plotted to highlight the trends.

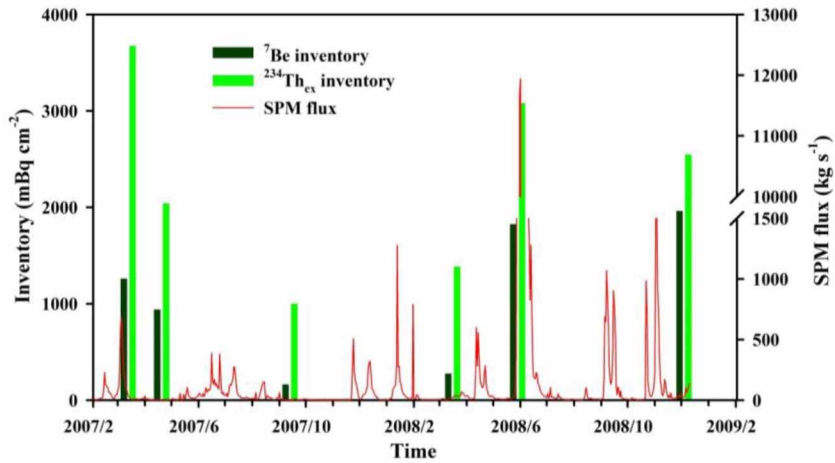
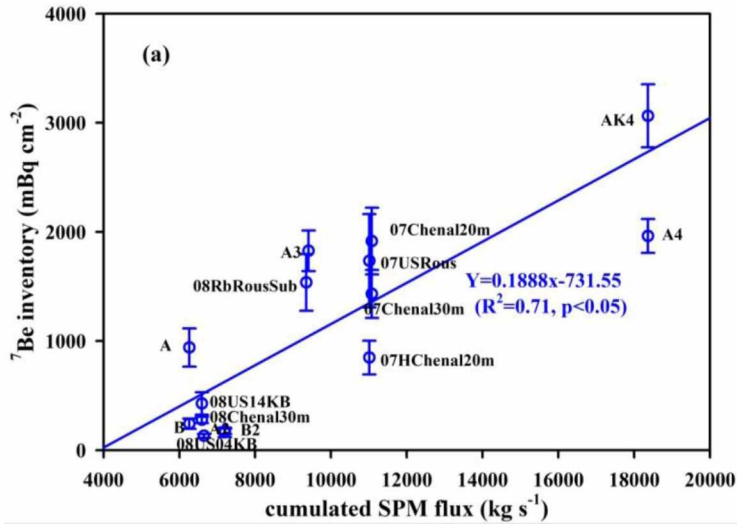
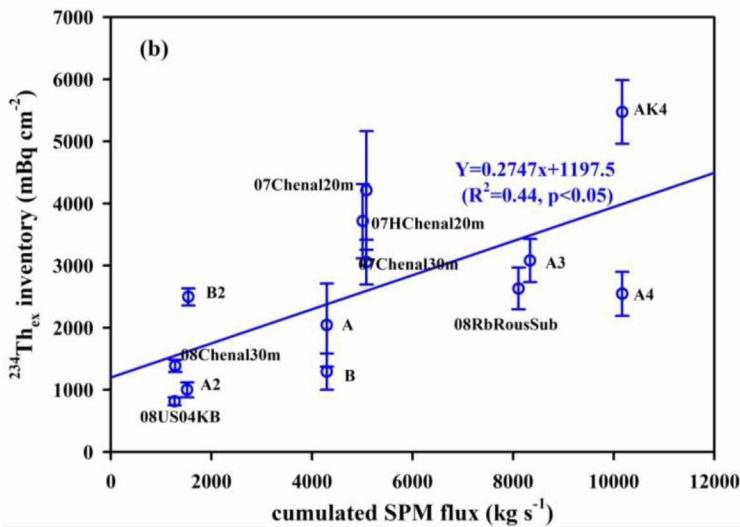


Figure 6. Temporal variations of ⁷Be and ²³⁴Th_{ex} inventories at Stn.A.

946
 947
 948
 949
 950
 951
 952
 953
 954



955



956

957

958

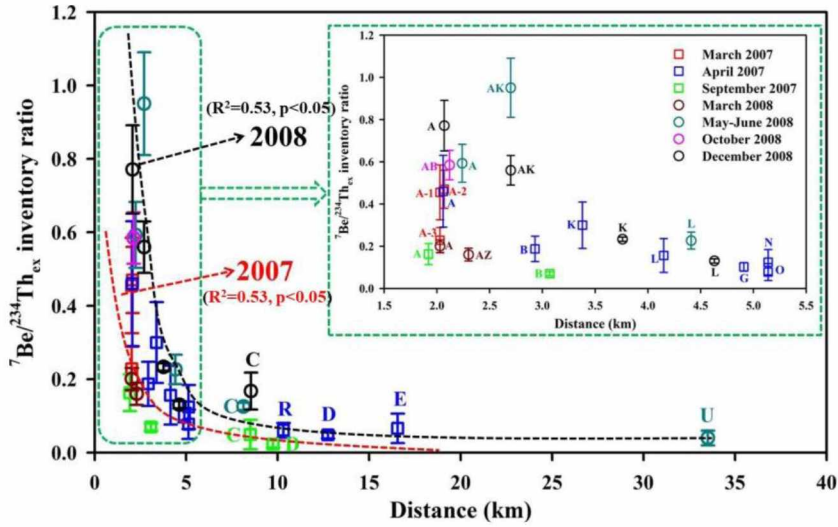
959

960

961

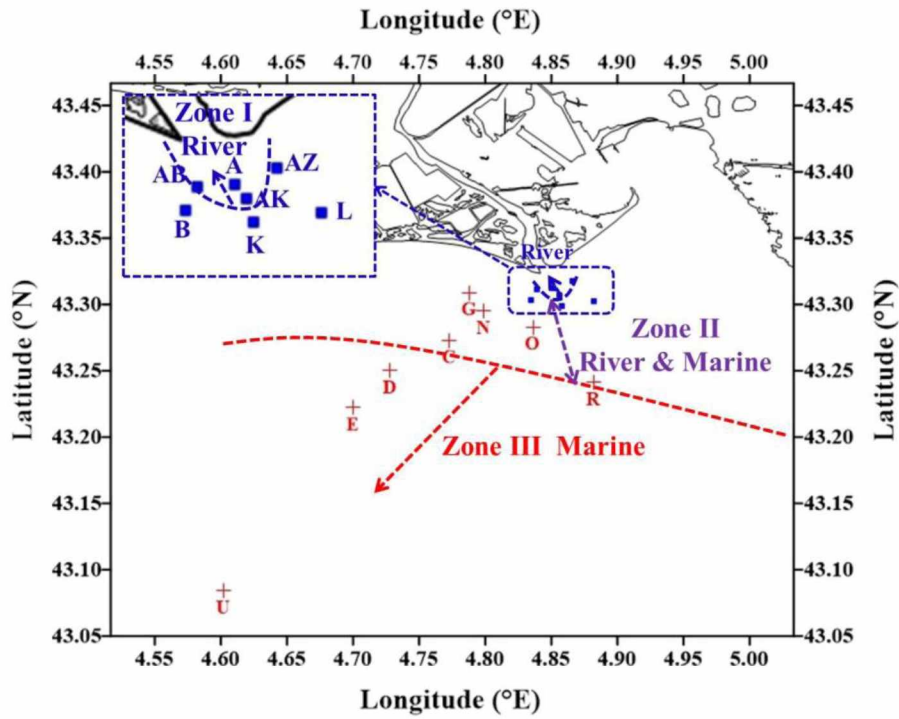
962

Figure 7. Relationship between ${}^7\text{Be}$ inventories in the Rhône River pro-delta and cumulated SPM fluxes calculated over 106 d (2 half-lives of ${}^7\text{Be}$) before the sampling date (a) excluding the Stn.AK3 collected in May-June 2008 flood; and relationship between the ${}^{234}\text{Th}_{\text{ex}}$ inventories in the Rhône River pro-delta and cumulated SPM fluxes calculated over 48 d (2 half-lives of ${}^{234}\text{Th}$) before the sampling date (b) excluding Stn.AK3.



964
 965
 966
 967
 968
 969
 970
 971
 972

Figure 8. ${}^7\text{Be}/{}^{234}\text{Th}_{\text{ex}}$ inventory ratio in sediment cores as a function of distance from the Rhône River mouth for March 2007 (red empty squares), April 2007 (blue empty squares), September 2007 (green empty squares), March 2008 (dark red empty circles), May-June 2008 (dark cyan empty circles), October 2008 (purple empty circles) and December 2008 (black empty circles). The exponential decreases of ${}^7\text{Be}/{}^{234}\text{Th}_{\text{ex}}$ inventory ratios with distance off the Rhône River mouth in 2007 and 2008 are plotted to highlight the trends.



973
 974
 975
 976
 977
 978
 979
 980
 981
 982
 983
 984

Figure 9. The zonation with different dominant sources of particles: input of river-borne particles (River) near the river mouth and marine particles (Marine) on the continental shelf.

Table 1. Sample information from selected stations of the Rhône River pro-delta sediments

Stations	Samples	Lat. (°N)	Long. (°E)	Depth (m)	Collection date (dd-mm-yyyy)	Measurement length (cm)	Distance (km) ^{a)}	Inventory	Data from Lab	
Southwest transect (SW)										
A	2007Chenal20m(-1)	43.311	4.853	28	13-03-2007	16	2.03	closed	IRSN/LMRE	
	2007Chenal30m(-2)	43.313	4.855	27	13-03-2007	16	2.07	closed	IRSN/LMRE	
2007HChenal20m(-3)	A	43.311	4.851	28	15-03-2007	14	2.03	closed	IRSN/LMRE	
	A	43.312	4.852	25	20-04-2007	16	2.06	closed	LSCE/LSM	
	A2	43.313	4.851	19	13-09-2007	7	1.92	closed	LSCE/LSM	
	2008Chenal30m	43.313	4.854	26	16-03-2008	15	2.03	closed	IRSN/LMRE	
	A3	43.310	4.851	32	29-05-2008	16	2.24	open	LSCE/LSM	
	A4	43.313	4.855	21	04-12-2008	12	2.07	open	LSCE/LSM	
	AB	2008US 14KB	43.312	4.835	26	16-03-2008	6	2.08	open	IRSN/LMRE
	2007US-Rous	2007US-Rous	43.310	4.841	27	15-03-2007	6	2.12	closed	IRSN/LMRE
2008RbRousSub		43.310	4.842	27	11-10-2008	13	2.12	closed	IRSN/LMRE	
AK	AK3	43.307	4.856	42	08-06-2008	38	2.70	closed	LSCE/LSM	
	AK4	43.307	4.856	46	04-12-2008	30	2.70	closed	LSCE/LSM	
AZ	2008US 04KB	43.318	4.866	25	15-03-2008	4	2.30	closed	IRSN/LMRE	
B	B	43.303	4.836	56	20-04-2007	10	2.93	closed	LSCE/LSM	
	B2	43.302	4.834	56	12-09-2007	7	3.07	closed	LSCE/LSM	
G	G	43.309	4.788	48	27-04-2007	6	4.91	closed	LSCE/LSM	
N	N	43.295	4.799	67	24-04-2007	5	5.14	closed	LSCE/LSM	
C	C2	43.272	4.772	75	14-09-2007	4	8.51	closed	LSCE/LSM	
	C3	43.274	4.776	75	30-05-2008	7	8.13	closed	LSCE/LSM	
	C4	43.273	4.770	72	04-12-2008	7	8.54	closed	LSCE/LSM	
D	D	43.250	4.728	74	23-04-2007	8	12.75	closed	LSCE/LSM	
	D2	43.301	4.728	72	14-09-2007	4	9.75	closed	LSCE/LSM	
E	E	43.222	4.700	75	21-04-2007	5	16.56	closed	LSCE/LSM	
U	U3	43.084	4.602	90	02-06-2008	1.5	33.51	closed	LSCE/LSM	
South transect (S)										

K	K	43.301	4.858	62	29-04-2007	9	3.38	closed	LSCE/LSM
	K4	43.296	4.852	67	03-12-2008	8	3.76	open	LSCE/LSM
O	O	43.283	4.836	79	24-04-2007	5	5.14	closed	LSCE/LSM
R	R2	43.241	4.882	98	28-04-2007	5	10.32	closed	LSCE/LSM
Southeast transect (SE)									
L	L	43.304	4.880	64	19-04-2007	7	4.15	closed	LSCE/LSM
	L3	43.303	4.883	65	01-06-2008	8	4.41	closed	LSCE/LSM
	L4	43.300	4.883	66	07-12-2008	6	4.63	closed	LSCE/LSM

986 a) This indicates the distance from the sampling station to the reference site (43.329°N, 4.842°E) in the Rhône River mouth.

987

988

989

Table 2. Inventories of ^7Be and $^{234}\text{Th}_{\text{ex}}$ in the Rhône River delta sediment cores and their $^7\text{Be}/^{234}\text{Th}_{\text{ex}}$ inventory ratios

Stations	Samples	Collection date (dd-mm-yyyy)	Cumulated SPM flux over 106 d ($\text{kg s}^{-1}\text{d}^0$)	Cumulated SPM flux over 48 d ($\text{kg s}^{-1}\text{d}^0$)	^7Be inventory (mBq cm^{-2})	$^{234}\text{Th}_{\text{ex}}$ inventory (mBq cm^{-2})	$^7\text{Be}/^{234}\text{Th}_{\text{ex}}$ inventory ratio
Southwest transect (SW)							
A	2007Chenal20m(-1)	13-03-2007	11080	5082	1915±306	4209±954	0.45±0.13
	2007Chenal30m(-2)	13-03-2007	11080	5082	1432±221	3055±362	0.47±0.09
	2007HChenal20m(-3)	15-03-2007	11013	5008	847±155	3715±597	0.23±0.06
	A	20-04-2007	6265	4296	940±175	2042±668	0.46±0.17
	A2	13-09-2007	7197	1518	163±43	1001±121	0.16±0.05
	2008Chenal30m	16-03-2008	6593	1281	277±29	1385±98	0.20±0.03
	A3	29-05-2008	9408	8336	1826±186	3081±348	0.59±0.09
	A4	04-12-2008	18364	10168	1963±155	2546±353	0.77±0.12
AB	2008US 14KB	16-03-2008	6593	1281	428±103	-	-
	2007US-Rous	15-03-2007	11013	5008	1735±428	-	-
	2008RbRousSub	11-10-2008	9350	8108	1537±260	2630±336	0.58±0.07
AK	AK3	08-06-2008	63216	59652	2797±275	2944±319	0.95±0.14
	AK4	04-12-2008	18364	10168	3064±289	5474±512	0.56±0.07
AZ	2008US 04KB	15-03-2008	6647	1268	130±18	814±65	0.16±0.03
B	B	20-04-2007	6265	4296	242±47	1294±292	0.19±0.06

	B2	12-09-2007	7204	1541	173±25	2496±137	0.07±0.01
G	G	27-04-2007	6101	895	134±21	1308±131	0.10±0.02
N	N	24-04-2007	6205	2169	74±23	599±196	0.12±0.06
C	C2	14-09-2007	7183	1496	41±32	837±142	0.05±0.04
	C3	30-05-2008	12919	11629	377±33	3000±204	0.13±0.01
	C4	04-12-2008	18364	10168	194±57	1156±153	0.17±0.05
D	D	23-04-2007	6215	2860	102±24	2118±159	0.05±0.01
	D2	14-09-2007	7183	1496	29±10	1237±83	0.02±0.01
E	E	21-04-2007	6268	3698	56±38	856±89	0.07±0.04
U	U3	02-06-2008	47852	45699	21±11	535±69	0.04±0.02
South transect (S)							
K	K	29-04-2007	5949	901	157±53	525±77	0.30±0.11
	K4	03-12-2008	18352	10149	741±23	3181±173	0.23±0.01
O	O	24-04-2007	6205	2169	113±51	1465±193	0.08±0.04
R	R2	28-04-2007	6052	712	52±15	850±76	0.06±0.02
Southeast transect (SE)							
L	L	19-04-2007	6278	3879	146±68	934±250	0.16±0.08
	L3	01-06-2008	35895	34019	459±70	2026±218	0.23±0.04
	L4	07-12-2008	18518	10352	294±13	2261±102	0.13±0.01

990 a) The cumulated SPM fluxes are calculated over 106 d (2 half-lives of ^7Be) before the sampling date.

991 b) The cumulated SPM fluxes are calculated over 48 d (2 half-lives of ^{234}Th) before the sampling date.

992

993

994

Table 3. Zoning in the Rhône pro-delta, where influences between river-borne particles and marine particles are dominant

Zone	Distance (km)	$^7\text{Be}/^{234}\text{Th}_{\text{ex}}$ inventory ratio	River vs. Marine
I	< 3.0	>0.50	River
II	3.0–8.5	0.10–0.50	River & Marine
III	>8.5	<0.10	Marine

995